nature reviews physics

https://doi.org/10.1038/s42254-024-00739-8

Review article

Check for updates

Experimental aspects of indefinite causal order in quantum mechanics

Lee A. Rozema [1,2,8] ✉, Teodor Strömberg [1,2,8], Huan Cao [1,2,8], Yu Guo [3,4,8], Bi-Heng Liu [3,4,5] & Philip Walther [1,2,6,7] ✉

Abstract

In the past decade, the toolkit of quantum information has been expanded to include processes in which the basic operations do not have definite causal relations. Originally considered in the context of the unification of quantum mechanics and general relativity, these causally indefinite processes have been shown to offer advantages in a wide variety of quantum-information processing tasks, ranging from quantum computation to quantum metrology. Here, we overview these advantages and the experimental efforts to realize them. We survey both the experimental techniques employed and the theoretical methods developed in support of the experiments, before discussing the interpretations of current experimental results and giving an outlook on the future of the field.

Sections

[1]Faculty of Physics, University of Vienna, Vienna Center for Quantum Science and Technology (VCQ), Vienna, Austria. [2]Research Platform for Testing the Quantum Gravity Interface (TURIS), University of Vienna, Vienna, Austria. [3]CAS Key Laboratory of Quantum Information, University of Science and Technology of China, Hefei, China. [4]CAS Center for Excellence in Quantum Information and Quantum Physics, University of Science and Technology of China, Hefei, China. [5]Hefei National Laboratory, University of Science and Technology of China, Hefei, China. [6]Institute for Quantum Optics and Quantum Information (IQOQI) Vienna, Austrian Academy of Sciences, Vienna, Austria. [7]Christian Doppler Laboratory for Photonic Quantum Computer, University of Vienna, Vienna, Austria. [8]These authors contributed equally: Lee A. Rozema, Teodor Strömberg, Huan Cao, Yu Guo.
✉e-mail: lee.rozema@univie.ac.at; philip.walther@univie.ac.at

Key points

- An indefinite causal order (ICO) is a situation wherein the order of different events or operations is placed in a quantum superposition. Thus one cannot ascribe a definite order to these operations.
- The best-studied process with an ICO is the quantum switch, which applies a set of quantum gates in a superposition of all possible permutations. The quantum switch has been experimentally implemented using various degrees of freedom encoded in single photons.
- There is a strong analogy between processes with an ICO and entangled states. This analogy can be used to design techniques to certify ICO.
- The quantum switch can be used to achieve advantages that go beyond devices that can be described by the quantum circuit model. Although there is no general computational advantage from the quantum switch, there are many specific applications, including quantum computation protocols, quantum communication, quantum metrology and even quantum thermodynamics.

Introduction

Quantum-information processing tasks are commonly described using the quantum circuit model, in which quantum states evolve through a series of gates applied in a fixed order. If one associates the application of the gates in such a circuit with events in space time, then the classically controlled order of these gates gives rise to a causal structure in which two events always have a definite causal relation, such as '*A* happened and then *B*'. By departing from the quantum circuit model, however, and instead using a quantum system to control the order of the gates, one arrives at quantum processes in which the constituent events do not have a definite causal structure. Events in such processes are said to have an indefinite causal order (ICO). Before going further, we stress that there are currently two distinct research lines in quantum foundations, which are both sometimes referred to as 'quantum causality'. The works we review here focus on one of these lines, namely, processes with an ICO, but there is also large body of work on what is known as quantum causal inference. In quantum causal inference, one studies correlations in multiparty networks. The goal is then to determine whether those correlations can be described classically, or if a quantum explanation, for example, based on entanglement, is required[1–6].

ICO processes were originally proposed in refs. 7,8 in the context of quantum superpositions of gravitational fields; ref. 9 was the first study from a pure quantum-information perspective, introducing the quantum switch: a process in which two gates U and V act in a superposition of causal orders, controlled by an auxiliary quantum system. This process was shown to strictly outperform any causally ordered circuit at the computational problem of determining whether a pair of gates commute or anti-commute, an advantage that was also demonstrated in ref. 10. Following the introduction of the quantum switch, ref. 11 generalized the process to scenarios involving more gates, whereas ref. 12 developed a framework to analyse processes with more general causal structures. This framework, the process matrix formalism (described in Box 1), was leveraged by ref. 13, which, in analogy to entanglement witnesses, introduced the notion of causal witnesses. Such a witness is an observable of a quantum process whose expectation value satisfies an inequality for all causally separable processes; that is, processes that can be described as probabilistic mixtures of processes with a definite causal structure. Armed with these tools, ref. 14, and later ref. 15, conclusively verified the indefinite causal structure of an experimental quantum process.

Following these initial studies, the potential of ICO processes was explored in various contexts. Reference[16] showed how an ICO process can achieve an exponential advantage in communication complexity for a tailored task, later realized in ref. 17; a quantum switch was used to show a universal protocol for time reversal[18]; ref. 19 applied ICO to quantum metrology and demonstrated super-Heisenberg sensitivity; and ref. 20 simulated an ICO-enhanced quantum refrigeration cycle, in which thermalizing channels bring a quantum system out of thermal equilibrium. This broad yet non-exhaustive set of experimental applications is a reason why ICO processes continue to attract attention within the field of quantum-information processing.

In this Review, we overview the current state of applications of ICO processes and survey the range of experimental methods used to realize them. We will also discuss methods used in the experimental characterization of ICO processes and explore loopholes in and criticisms of the experimental demonstrations performed thus far. Although early experimental results in the field were previously reviewed[21], we aim to provide a broader and more holistic view of the experimental aspects of indefinite causality in quantum mechanics. Finally, as a comprehensive theoretical introduction to indefinite causality is beyond our scope, we instead refer interested readers to ref. 22.

Experimental realizations of ICO

Most experimental work on ICO has focused on the two-party quantum switch. This is a two-qubit process consisting of a control qubit C and a target qubit T. The quantum switch then takes two gates U and V, applying them in a superposition of both orders to the target qubit, in which the precise superposition is dependent on the state of the control qubit as:

$$(U, V) \mapsto U_T V_T \otimes |0\rangle\langle 0|_C + V_T U_T \otimes |1\rangle\langle 1|_C. \quad (1)$$

To date, all physical realizations of this process have encoded both the target and control systems in the same particle, specifically using two different degrees of freedom (DoFs) of a single photon. As every localized optical device can be thought of as performing a controlled operation conditioned on the path of a particle, passing through the device or not, controlled operations between any two internal DoFs can be realized by first mapping one of these to the photon path (Fig. 1a, top). This insight, which underlies all the experiments discussed here, was first hinted at in ref. 23, in which the authors proposed a scheme for probabilistically determining whether two unitaries commute. The coherent unitary control needed for ICO processes was first realized in ref. 24, in which the authors experimentally transformed a black-box unitary into a controlled version of itself (Fig. 1b, top), a task later shown to be forbidden in the quantum circuit model[25]. Building upon these two works, it was subsequently shown how to control the order of two gates in a photonic setting[26,27].

The first experiments on ICO used a modified version of the scheme from ref. 23 to deterministically superpose gate orders using a path control qubit and a polarization target system[10,14]. Follow-up experiments, however, have made use of a multitude of encodings, and

Box 1 | Process matrices

A valuable toolkit to describe processes exhibiting an indefinite causal order and to capture their temporal correlations is the process matrix formalism. In this framework, quantum mechanics is assumed to be valid locally, without referring to the existence of a global causal structure[12]. The process matrix formalism aims to characterize probability distributions in scenarios involving the application of local operations. Generally, these operations, encompassing deterministic processes such as unitaries, quantum channels or generalized measurements, are described by completely positive trace non-increasing maps $\mathcal{M}^A : \mathcal{L}(\mathcal{H}^{A_I}) \to \mathcal{L}(\mathcal{H}^{A_O})$, in which $\mathcal{L}(\cdot)$ denotes the space of linear operators over the input (output) Hilbert spaces $\mathcal{H}^{A_I}$ ($\mathcal{H}^{A_O}$). The completely positive map $\mathcal{M}_a^A$ is often associated with an outcome a, and its representation is facilitated by the Choi–Jamiołkowski isomorphism[172,173]. The Choi–Jamiołkowski matrix $M_a^{A_I A_O}$ corresponding to $\mathcal{M}_a^A$ is defined as:

$$M_a^{A_I A_O} := \mathcal{I} \otimes \mathcal{M}_a^A(|\mathbb{1}\rangle\rangle\langle\langle\mathbb{1}|) \in \mathcal{L}(\mathcal{H}^{A_I}) \otimes \mathcal{L}(\mathcal{H}^{A_O}), \tag{2}$$

in which $\mathcal{I}$ is the identity map and $|\mathbb{1}\rangle\rangle = \sum_j |j\rangle^{A_I} \otimes |j\rangle^{A_I} \in \mathcal{H}^{A_I} \otimes \mathcal{H}^{A_I}$. The collection $\mathcal{J}_A = \{\mathcal{M}_a^A\}$ associated with all outcomes must fulfil the condition that $\sum_a \mathcal{M}_a^A$ is completely positive and trace-preserving.

The key element of this formalism is the process matrix W, used to compute the probability to obtain the outcomes $a_1, a_2, \ldots, a_N$ under the completely positive maps $M_{a_1|x_1}^{A_I^1 A_O^1}, \cdots M_{a_N|x_N}^{A_I^N A_O^N}$ for a choice of operations $x_1, x_2, \ldots, x_N$ via Born's rule written in process matrix notation:

$$P\left(M_{a_1|x_1}^{A^1} \cdots M_{a_N|x_N}^{A^N}\right) = \mathrm{tr}\left[\left(M_{a_1|x_1}^{A_I^1 A_O^1} \otimes \cdots \otimes M_{a_N|x_N}^{A_I^N A_O^N}\right)^{\mathrm{T}} W\right], \tag{3}$$

in which $W \in \mathcal{L}(\mathcal{H}^{A_I^1} \otimes \mathcal{H}^{A_O^1} \otimes \cdots \mathcal{H}^{A_I^N} \otimes \mathcal{H}^{A_O^N})$ is a Hermitian operator and $()^{\mathrm{T}}$ is the transpose. This process matrix W can be seen as a generalization of a density matrix, and the previous equation serves as a generalization of Born's rule. This framework extends the formalism of the 'quantum comb'[174].

In the bipartite scenario involving parties A and B, a process matrix W_{sep} is called causally separable if it can be expressed as a convex combination of causally ordered processes, that is, $W_{\mathrm{sep}} = pW^{A\preccurlyeq B} + (1-p)W^{B\preccurlyeq A}$, in which $W^{A\preccurlyeq B}$ describes the process in which the actions of party A causally precede those of party B and $0 \le p \le 1$. Concretely for the quantum switch in the bipartite case, with the control qubit initialized in $\frac{1}{\sqrt{2}}(|0\rangle + |1|)^C$, the process matrix is represented by $W_{\mathrm{switch}} = |w_{\mathrm{switch}}\rangle\langle w_{\mathrm{switch}}|$, with the process vector

$$|w_{\mathrm{switch}}\rangle = \frac{1}{\sqrt{2}}\left(|w^{A\preccurlyeq B}\rangle|0\rangle^C + |w^{B\preccurlyeq A}\rangle|1\rangle^C\right), \tag{4}$$

$$|w^{A\preccurlyeq B}\rangle = |\mathbb{1}\rangle\rangle^{\mathcal{H}^{\mathrm{in}} A_I}|\mathbb{1}\rangle\rangle^{A_O B_I}|\mathbb{1}\rangle\rangle^{B_O \mathcal{H}^{\mathrm{out}}}, \tag{5}$$

and $|w^{B\preccurlyeq A}\rangle$ is similarly defined. The illustration shows the process matrix of the two-party quantum switch. Depending on the formulation, $\mathcal{H}^{\mathrm{in}}$ and $\mathcal{H}^{\mathrm{out}}$ can refer to the control system, the target system or both. Here, $\mathcal{H}^{\mathrm{in}}$ ($\mathcal{H}^{\mathrm{out}}$) is associated with the Hilbert space of the input (output) space of quantum switch.

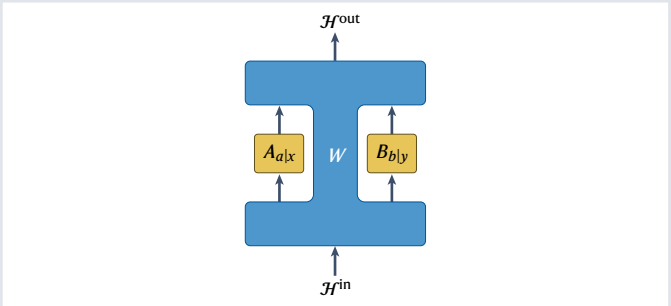

ICO processes have been demonstrated using a polarization control and transverse-electric mode (TEM) target system[15,28], propagation-direction control and time-bin target[17], propagation-direction control and polarization target[18,29,30], time-bin control and polarization target[31], and even path control and a continuous variable target[19]. These different encodings will be examined subsequently.

Path control

To date, the majority of quantum switch realizations have used the path DoF of single photons as the control system. This is a natural choice, as, as discussed, any optical device can be interpreted as a controlled operation between the position of the device and the photonic DoF that it acts on. A coherently controlled operation with a qubit control system can, therefore, be realized by a superposition of two optical paths, one passing through the optical device and one bypassing it, as illustrated in the top panel of Fig. 1a. Similarly, the order of two quantum operations can be controlled by aligning two paths of a photon such that they pass through the optical devices in opposite orders (bottom panel of Fig. 1a). More complex superpositions of orders of operations can be realized by increasing the number of paths over which the photon is superposed.

Polarization target. The first realization of a quantum switch used the polarization state of a single photon to encode the target system[10]. A balanced beam splitter was used to prepare a superposition of two photon paths, which were aligned to propagate through two sets of three wave plates in two different orders. The experiment demonstrated the ability of the quantum switch to determine whether two gates U and V, realized by the two sets of wave plates, commute or anti-commute with unity success probability, thereby indirectly serving as a witness for an ICO. The key difference with respect to the probabilistic approach of ref. 23 was the use of a folded Mach–Zehnder interferometer (MZI) geometry, in which both arms of the interferometer were made to propagate through both unitary transformations, but in different orders. This alignment necessitates two different paths through the polarization optics black boxes implementing U and V, which requires these elements to be spatially uniform, and has additionally been a source of discussion about the interpretation of the experiment (see the section on loopholes for more details). The commutator was measured by projecting the control system in equation (1) on $\{(|0\rangle \pm |1\rangle)/\sqrt{2}\}$ using the second beam splitter of the MZI, followed by non-polarization-resolving detection of the photon path. Pairs of gates that anti-commute have

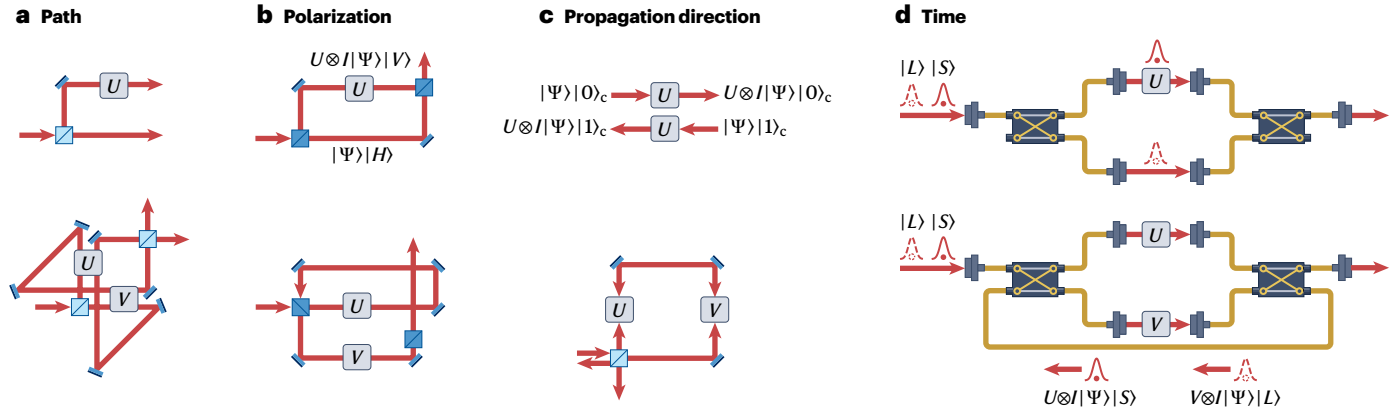

Fig. 1 | Different control state encodings to realize the quantum switch. Four different photonic control-state encodings that have been used to demonstrate indefinite causal processes. **a**, Top: a balanced beam splitter can prepare a superposition of path-encoded control states. In the upper path, the unitary U is applied to the internal target system, whereas in the lower path the identity operation I is applied to the target. Bottom: these outputs of the beam splitter can be aligned to propagate through two unitary channels (U, V) in different orders, thereby realizing a quantum switch. **b**, Top: a polarizing beam splitter (PBS) maps a polarization-encoded control qubit state (H, V) to a path state, enabling coherent unitary control. The second PBS recombines the path degrees of freedom. Bottom: by connecting the output of the second PBS to the input of the first, a quantum switch can be realized. **c**, Top: in this realization, the physical device is designed to apply U when the photon traverses it in either direction. Bottom: connecting the two outputs with a beam splitter forms a closed path with two propagation directions. Placing two unitary channels in this path naturally correlates the propagation direction with the gate order, thereby generating a quantum switch. **d**, Top: in a time encoding, the control state is prepared in a superposition of time bins by passing through a short $|S\rangle$ or long $|L\rangle$ delay line. Ultrafast optical switches are used to perform controlled unitaries, by only routing the $|S\rangle$ state through the unitary channel. Bottom: a quantum switch can be constructed by routing one output of the second optical switch to the first.

the effect of introducing a relative π phase between the two interferometer arms, thereby performing a SWAP operation on the output ports when the interferometer is balanced. However, as the information about the commutativity of the two gates is encoded in the interference condition, such an interferometer cannot be stabilized by classical light co-propagating through the polarization optics. The experiment, therefore, instead utilized passive phase stabilization in concert with a lock-and-hold technique. Several subsequent experiments adopted the methods of ref. 10 to other realizations of ICO processes[14,20,32–37]. In refs. 20,34,35, the problem of phase stability was addressed by actively locking the interferometer using a carefully aligned laser beam so that it co-propagated with the single photons without being subjected to the polarization rotations inside the quantum switch.

Polarization control

There have been several demonstrations of ICO processes using the polarization DoF for the control system, and these experiments are based on the idea of refs. 24,25 to use a birefringent element to entangle the photon polarization with the photon path, performing the target operations on an additional DoF conditioned on the path and finally disentangling the polarization and path, as shown in Fig. 1b. In these experiments, only a single path passes through each optical element, in contrast to situation with a path-control qubit. Nevertheless, the target operations are still applied on two orthogonal optical modes (polarization in this case).

TEM target. The first experiment to make use of a polarization-encoded control system was the measurement of a causal witness[15] (discussed in detail in the next section). In this experiment, the target system was encoded in the two Hermite–Guassian modes HG_{01} and HG_{10} of the transverse electric field, which forms a 2D subspace of the space of TEMs. The setup consisted of a polarizing beam splitter (PBS)-based MZI that was traversed twice, cancelling any phases owing to path-length fluctuations and removing the need for stabilization of the setup. The transformations of the target-state TEMs were realized using a set of inverting prisms and cylindrical lenses and, in contrast to the experiments using a path polarization encoding, the two control qubit states could be made to fully overlap inside the devices realizing the transformation. These advantages come at the cost of optically more complex target-state transformations, making high-fidelity operation challenging. This, however, did not stand in the way of follow-up work using the same methods to demonstrate communication through a depolarizing channel[28].

Continuous-variable target. The polarization control system was also used together with a continuous-variable target to demonstrate super-Heisenberg quantum metrology[19]. For this task, the different evolutions of the target had to satisfy the Weyl relation[38], which is not possible in a discrete variable system. Thus, the target system was taken to be the transverse coordinate of the photon, and the evolutions were taken to be position and momentum displacements. The position displacement was realized using 2 mm thick birefringent MgF_2 and the momentum displacement was realized using an optical wedge pair. A challenge in this experiment was to precisely calibrate the direction of the beams in each path to ensure that they strictly propagated along a predefined axis. The directions of the beams were aligned with a deflection angle that was two orders of magnitude lower than that introduced by the displacements. This was achieved by controlling the fluctuations of the beam position to within less than 5 µm along a 4 m calibration optical path. The ability to use essentially the same apparatus to encode both discrete-variable and

continuous-variable systems highlights the flexibility of photonic quantum switches.

Propagation-direction control

Instead of encoding the control system in two distinct photon paths, there have also been experiments that encoded this system in two different propagation directions along the same optical path. For the two-party quantum switch, shown in Fig. 1c, such a configuration automatically generates the superposition of gate orders and furthermore bestows an insensitivity to path-length fluctuations as the two control system states traverse the same path. A challenge associated with this approach is that the black boxes acting on the target state have to be invariant under the reversal of propagation direction.

Time-bin target. The first experiment to make use of a propagation-direction encoding of the control system was a demonstration of an exponential communication advantage using an ICO[17]. This task required a bit string to be encoded in the target system, which therefore had to be high dimensional. This made time bins a suitable choice, as the encoding can in principle be extended indefinitely. The operations implemented in the experiment consisted of shift operations in the computational (time-bin) basis, as well as time-bin-dependent phase shifts. The former was realized using high-precision fibre patch cables, and the latter used two fast phase modulators. Through the use of fibre delays, these modulators acted independently on photon wave packets in the two different propagation directions, and these decoupled operations could therefore be chosen to be identical.

Polarization target. The transformations generated by standard polarization optics, such as wave plates, are not fully invariant under reversal of the propagation direction. However, there exists a subset of polarization rotations in SU(2) that is invariant for such devices. Thus, this encoding is especially suitable for applications of the quantum switch that do not strictly require a universal qubit-gate set, such as a time-rewinding protocol[18] and an ICO version of Deutsch's algorithm[30]; both of which have been demonstrated. At the cost of more complex polarization black boxes, it is possible to realize fully invariant transformations and, therefore, a quantum switch with propagation-direction control with a universal gate set[29]. However, the passive phase stability comes at a cost; in particular, the fixed interference condition ensured by the Sagnac geometry restricts the range of possible control-qubit measurements when only using passive optical elements.

Time-bin control

The temporal DoF of photons has the attractive property of being largely decoherence-free, as co-propagating temporally offset single-photon wave packets do not acquire relative phase, while also offering a large Hilbert space. This property was exploited in ref. 17 to encode a large target system, but could also be leveraged for a high-dimensional control system to realize superpositions of gate orders beyond the two-party quantum switch as was proposed in ref. 39. To date, there has only been a single demonstration of a quantum switch using a time-bin control system[31], likely due to the complexities associated with manipulating and measuring time-bin qubits. When measuring a time-bin state in a superposition basis, care must be taken that the measurement apparatus shares a phase reference with the state-creation stage. The experiment presented in ref. 31 tackled this challenge by reusing the state-generation stage for the measurement of the control qubit, thereby ensuring a vanishing phase difference. However, similar to the case of propagation-direction control, without the use of fast phase modulators this limited the measurements of the control system to the σ_z and σ_y bases. The target state was encoded in the polarization DoF and controlled operations between the control and the target were realized using ultrafast optical switches that actively routed the light through the polarization optics in two different orders. This is illustrated in Fig. 1d. The experimental apparatus was used to perform tomography on the quantum switch and reconstruct the process matrix. This protocol measured 9,216 different probabilities, which required the experiment to remain stable for ~24 h and thus demonstrated the utility of passively stable platforms.

Variations on the quantum switch

The experiments described earlier have all been realizations of the two-party quantum switch with qubit control systems and were restricted to unitary operations on the target system. Although the quantum switch is uniquely defined by its action on unitary transformations[40], it remains a valid supermap for non-unitary transformations as well, and there have been several experiments demonstrating this[14,28,31,32,34,35]. Additionally, ICO processes with higher-dimensional control systems have been studied extensively from a theoretical perspective[41–43], and one such process has been the subject of an experiment[44].

High-dimensional control systems. For pairs of gates, the quantum switch can efficiently answer the computational question of whether the gates commute, but when considering more than two gates this is no longer a well-posed question. However, there are analogous problems for $2^k = N$ permutations of N qubit gates, called Hadamard promise problems[44]. An instance of such a problem for $N = 4$ was solved using a simplified version of the four-party quantum switch in ref. 44, which superposed only 4 of the possible 24 orders of the gates. The experiment used a path (polarization) control (target) encoding, which lends itself well to higher-dimensional control systems as the number of photon paths can, in principle, be extended arbitrarily. However, a direct extension of the approach pioneered in ref. 10 leads to prohibitively complex optical geometries for higher-dimensional control systems. The experiment, therefore, instead used multicore fibres to multiplex several modes through a single fibre, and the polarization optics acting on the target state were placed in the Fourier plane of the fibre launchers to ensure spatial overlap of the four modes. The initialization and measurement of the four-level control system (ququart) were performed using four-core fibre beam splitters realizing Hadamard transformations[45].

Non-unitary operations in the quantum switch. Indefinite causal processes involving non-unitary operations have been demonstrated for various different quantum channels. The first of these to be realized were measure-and-reprepare channels, which can be performed as a von Neumann measurement in which detection is delayed until after exiting the quantum switch to maintain coherence. For polarization target encodings, such measurements were realized using a PBS[14] and in ref. 35, two measurements were performed using beam displacers. In both cases, the measurement outcome is encoded in the photon path, thereby doubling the number of paths with each measurement. For experiments that do not encode the control system in the photon path, this presents a problem, and the time-bin-control experiment in ref. 31 solved it by only recording one measurement outcome at a time.

A second type of non-unitary quantum channel that has been realized inside a quantum switch is a decohering or depolarizing channel.

In two experiments using polarization[34] and TEM[28] target-state encodings, such channels were realized by exploiting the fact that they can be decomposed as mixtures of unitary Pauli channels. The decoherence then emerges in the data analysis through an appropriate averaging of measurement outcomes for the different Pauli channels. In a subsequent experiment[32], polarization-encoded target states were decohered by rapidly modulating the unitary channel using liquid crystal retarders. The timescale of this modulation was not fast enough to randomize the transformation on a shot-to-shot basis, but was nevertheless fast enough to attribute the bulk of the decoherence to the channel rather than the post-measurement averaging.

Yet another example of a non-unitary channel implemented in a quantum switch is amplitude damping[20], which was studied in the context of ICO in quantum thermodynamics, in a realization of a quantum refrigeration protocol proposed in ref. 46. Similar to the realizations of decohering channels, the generalized amplitude damping channel can be decomposed into pairs of Kraus operators, and classical averaging over these channels produces the desired map. The Kraus operators in the decomposition are themselves non-unitary maps and were realized on the polarization target system through two MZIs embedded inside the quantum switch. The non-trace-preserving nature of the Kraus operators manifests as loss when the photon exists in an output of the MZI that is not collected. Similar methods, using beam-displacer polarization MZIs, were applied in ref. 36 to realize a non-unitary process to charge a quantum mechanical system, that is used to store energy (a quantum battery), in terms of its Kraus operators.

The quantum switch in non-photonic platforms. There have been two experiments on ICO with matter-based qubits, specifically superconducting qubits[47] and an NMR system[48]. These platforms differ from the photonic ones previously discussed in that they only have a single experimentally accessible DoF, and consequently the gate order cannot be coherently controlled. Although future experiments using matter-based qubits may make use of coherent unitary control, as it has been shown to be possible for ion-based systems[27], the two experiments discussed here instead implemented circuit-model simulations of the ICO processes in which each quantum channel is realized twice. In the superconducting experiment[47], the quantum refrigeration cycle proposed in ref. 46, which was also the subject of ref. 20, was used to bring a qubit state out of equilibrium with two reservoirs using only thermalizing channels. These channels were implemented unitarily as SWAP operations with randomly drawn qubit states in the reservoir, and the thermal ensembles were realized using classical averaging of measurement outcomes. A modified version of the refrigeration protocol was demonstrated in an NMR platform[48]. In contrast to the pure states used in ref. 47, the qubits representing the thermal reservoirs were decohered using magnetic field gradients as part of the experimental state initialization.

Experimentally implemented processes aside from the quantum switch

The experiments discussed so far all fit within the framework of indefinite causality and can be accurately described using the process matrix formalism (described in Box 1). However, processes that go beyond this framework have been proposed. The first such process is a map that acts on a quantum channel[49] and transforms it into a coherent superposition of itself and its transpose or its adjoint. As the transpose or the adjoint of a channel can be understood as its time reversal, this process has been dubbed the quantum time flip[49]. Unlike the quantum switch, this is only valid for a subset of quantum channels; namely, the set of unital channels, which is the set of linear combinations of unitary channels[50]. These channels are said to be bidirectional. A composition of two time flips can outperform any causally ordered process, and even any process captured by the process matrix formalism, in a specific channel discrimination task. This advantage has been witnessed experimentally[51,52] using polarization-encoded target states and methods similar to those used in realizations of the quantum switch. In ref. 51, the time flip was realized on unitary transformations by exploiting the basis-dependent nature of the transposition operation, and in ref. 52, the time flip was applied to measure-and-reprepare channels with a single outcome, analogous to ref. 31. A theoretical study of the applicability of the time flip to communication tasks has also been carried out[53].

Processes without a known implementation

Although this Review focuses on experimentally realized processes with an ICO, it would not be complete without mentioning more general processes. In Box 1, we introduce the process matrix formalism, following the seminal work of ref. 12. This formalism can be used to describe scenarios wherein quantum theory is assumed to hold in different local laboratories, but without making any assumptions about the causal order between these laboratories. Using process matrices, the authors of ref. 12 introduced causal inequalities (discussed in the next section) and processes, which can violate them. Such processes arguably possess a stronger form of ICO than the quantum switch, as it is known that the switch cannot violate causal inequalities[13,54]. The best-known process is now called the OCB process, after Oreshkov, Costa and Brukner, the authors of ref. 12. Although it is not known whether the OCB process can be experimentally implemented, it, and other similar processes[55–59], remains a topic of theoretical investigation.

Characterizing ICO

So far, we have discussed ICO in a rather qualitative manner, that is, a process with an ICO is one wherein it cannot be said if A occurs before or after B. This notion has been rigorously formalized, based on the process matrix formalism, introduced in Box 1. In brief, one can use the Choi–Jamiołkowski isomorphism to consider quantum processes as quantum states. On the basis of this, one can then define causally separable processes as those with a well-defined causal order and causally non-separable processes as those with an ICO. The mathematics behind this approach is analogous to those describing separable and entangled states, allowing for the adaptation of a host of tools, originally designed for entanglement certification, to the problem of characterizing ICO. Similar to entanglement certification, ICO certification can be performed with device-dependent (DD), semi-device-independent (semi-DI) or fully device-independent (DI) methods (represented in Fig. 2). Historically, the first proposal for ICO verification was a DI technique known as a causal inequality[12]. However, an experimental DI verification has not yet been performed. On the one hand, this is because it is not known if the process required to implement the best-known DI technique — causal inequalities — can be physically implemented. On the other hand, new research has led to DI techniques based on the quantum switch[60,61], and it is likely a matter of time before they are experimentally implemented. Thus, we will first discuss DD ICO characterization techniques, then theory-independent and semi-DI

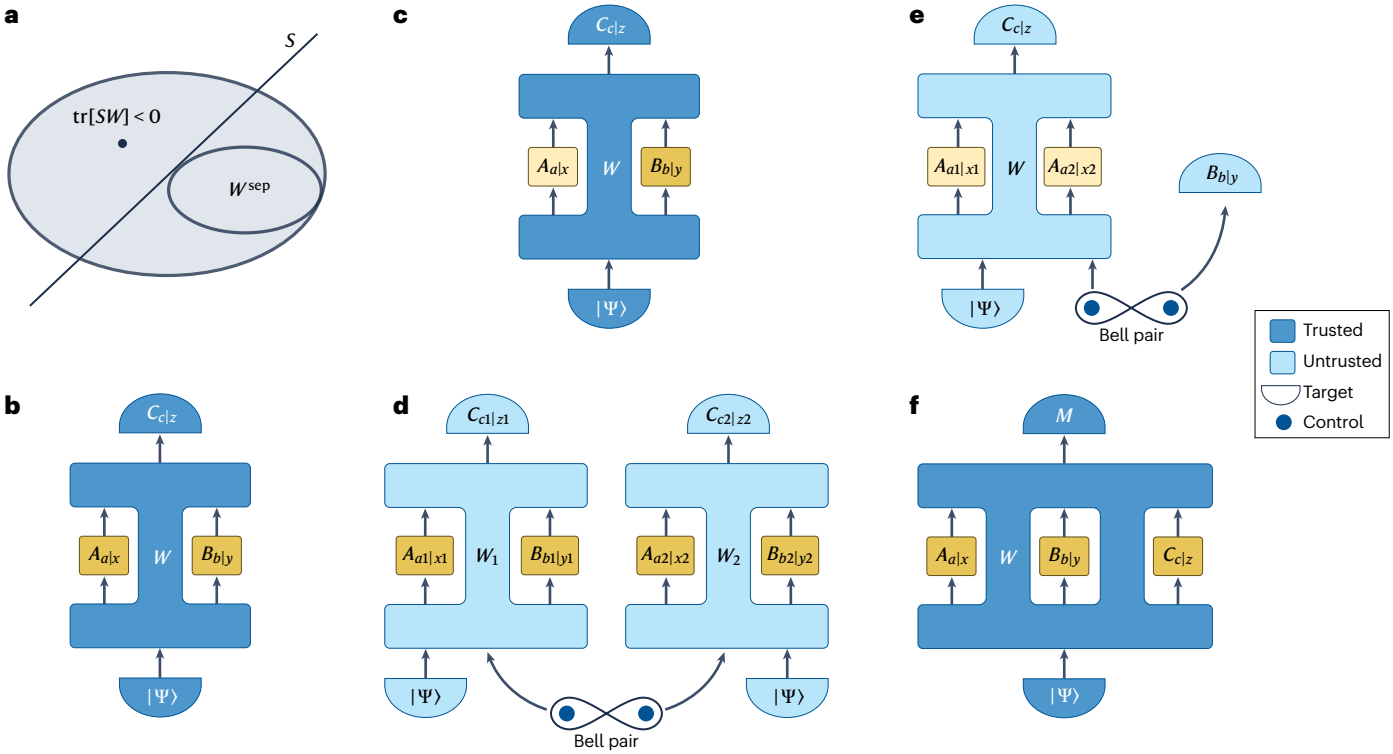

Fig. 2 | Certification of indefinite causal order. The darker-filled areas represent trusted devices, whereas lighter-filled areas are untrusted. Process matrices are represented as the blue areas labelled with W. Quantum instruments, represented by square boxes filled with yellow, are considered as inputs for process matrices. Note that the dark/light shading applies both to the blue process matrices and the yellow instruments. The instruments are labelled as $Q_{i|j}$, in which Q describes the location in the process matrix, j labels channel implemented by that party and i is the output of that channel (if it has one). The upper semicircles represent the measurement with the indicated instrument, and the lower semicircles are the preparation of quantum states $|\psi\rangle$. **a**, The causal correlations for causally separable processes W^{sep} are depicted by a convex set. A hyperplane S, representing a causal witness, separates causally separable processes. Negative values of $\text{tr}[SW] < 0$ signify that W is causally non-separable. **b**–**e**, Evaluation of causal non-separability in different scenarios. The distinction between full device dependence (part **b**) and other scenarios is given by which instruments within the quantum switch W are trusted and which are untrusted. **c**, One example of semi-device-independent certification where A is untrusted. **d**, Theory-independent protocol to verify an indefinite causal order, wherein the control qubits of two switches are entangled. For this panel only, the lighter-filled areas represent components that are not assumed to be described by the quantum theory. This approach is not device-independent, as it requires specific properties of the initial states and laboratory operations to be verified. **e**, Device-independent approach using ancillary distributed entanglement and space-like-separated observers. The control qubit of the quantum switch is entangled with an ancilla qubit. **f**, High-dimensional switch allowing the order of additional parties to be superposed.

techniques, and conclude this section with an outlook discussing DI proposals, including the aforementioned causal inequality.

Device-dependent techniques

Causal witnesses. Causal witnesses were developed to verify an ICO[13] and are somewhat analogous to entanglement witnesses. They are a DD ICO characterization method and were one of the first techniques for verifying an ICO to be experimentally implemented[14,15]. In the case of a process with two parties, Alice (A) and Bob (B), the goal is to determine whether there is a well-defined causal order between them. This is defined as one of the three following scenarios: the target system is sent first to A and then to B, first to B and then to A, or the process is a convex mixture of those two scenarios. Using the Choi–Jamiołkowski isomorphism to describe a quantum process matrix W as a quantum state, two fixed order processes $W^{A\preccurlyeq B}$ and $W^{B\preccurlyeq A}$ can be defined. One can employ the separating hyperplane theorem (Fig. 2a) to distinguish causally non-separable processes ($W^{\text{non-sep}}$) from causally separable processes: the aforementioned convex mixtures: $W^{\text{sep}} = pW^{A\preccurlyeq B} + (1-p)W^{B\preccurlyeq A}$. A causal witness, then, is a Hermitian operator S whose expectation value is negative $\text{tr}[SW^{\text{non-sep}}] < 0$ only if the process matrix is causally non-separable. The interpretation of the actual value of this expectation value is somewhat subtle and depends on the precise normalization of S. Some refer to it as the 'causal non-separability' (CNS) $\text{tr}[SW^{\text{non-sep}}] :=$ CNS (ref. 14). The CNS is related to how much noise a given witness can tolerate and still detect the presence of an ICO and is sometimes also called 'robustness'[31].

We mentioned that measuring a causal witness requires one to measure the expectation value of a quantum process. Although one does not typically discuss the expectation values of processes, this concept is mathematically well defined as the Choi–Jamiołkowski isomorphism allows one to consider quantum processes as states. Experimentally measuring a causal witness requires one to decompose the witness in terms of operations that are accessible in the laboratory. This is similar to how one measures an entanglement witness by decomposing it in terms of local measurements. The causal witness procedure is represented in Fig. 2b, in which the solid blue area labelled W

represents the unknown process matrix we wish to characterize. Then to assess the ICO of W, one must vary the input states (labelled $|\psi\rangle$), the post-process measurements (labelled $C_{c|z}$) as well as channels of Alice and Bob (labelled $A_{a|x}$ and $B_{b|y}$, respectively). Here, $x(y)$ refers to the specific channel chosen and $a(b)$ is the output (if any) of the given channel. The operations of Alice and Bob can be unitary gates, quantum channels, positive operator-valued measures or measure-and-reprepare instruments[62]. The precise choice of channels will affect the maximum obtainable value of the CNS, and not all sets of operations can be used to detect an ICO.

The first experimental proof of a causally non-separable process using a causal witness was reported in ref. 14. In this work, to achieve a larger CNS, one of the parties in the switch was equipped with a measure-and-reprepare channel, as discussed before. The work also represents the first time a non-unitary operation was placed in an ICO process. Shortly after, the violation of a causal witness using only unitary operations was also demonstrated[15]. The violation of a similar unitary-only witness, formulated using the methods developed in ref. 63, was later shown in ref. 29. In this context, it is also worth pointing to ref. 31. Although this work focused on experimentally performing process tomography on the quantum switch, it also discusses the measurement of different causal witnesses on the switch; in particular, witnesses constructed using different sets of channels and normalized differently to represent different notions of robustness.

Multipartite causal witnesses. Although most investigations of ICO have focused on bipartite cases, one can also define ICO for multipartite cases (those involving more than two parties). This situation is similar to that of multipartite entanglement; wherein, multipartite states have a much richer state-space structure, leading to different classes of entanglement[64,65].

For ICO, consider, for example, the case of three parties A, B and C (Fig. 2f). If one can group specific subsets of parties together and ascribe a well-defined order of the subsets to other parties, then this would not constitute a genuine multipartite non-causal correlation. For example, if B and C are grouped together as a new party, and then A occurs in their causal past, then this is not multipartite ICO even if B and C are causally non-separable. Thus, genuine multipartite ICO should exclude the existence of partial causal orderings and specify a given correlation for which no subset of parties can be grouped as mentioned earlier. This idea has been formalized in several theoretical studies[41–43]. Experimentally studying this problem with currently accessible methods requires one to incorporate N parties in quantum switch, that is, to build a quantum N-switch. As discussed before, a process similar to the four-switch, wherein a subset of all possible orders were superposed, has been experimentally realized[44]. This work demonstrated the computational advantages of a Hadamard promise problem, involving four unknown unitary gates. However, the number of settings required to implement the four-partite witness was prohibitively high and prevented the authors from verifying a multipartite ICO. Nevertheless, the study provides a recipe to create a multipartite causal witness for their process.

Process matrix tomography. Process matrices represent so-called higher-order quantum processes. This naming reflects the fact that they can take as input both quantum states and quantum operations and can return states, operations or both. In particular, for the quantum switch, the channels of Alice and Bob are said to be the inputs to the process.

Given that to fully characterize a higher-order process, one must input a complete set of operations for each input channel, the scaling of higher-order process tomography is even worse than that of standard process tomography. To practically combat this challenge, ref. 31 constructed a passively stable fibre-based quantum switch, to facilitate the required large number of measurements. Complete higher-order process tomography would have required the measurement of 13,824 different probabilities to reconstruct the process matrix of the two-party quantum switch. However, owing to experimental limitations in measuring the time-bin control system, the experiment used additional constraints and only measured 9,216 different probabilities[31]. This work represents the first experimental technique to completely characterize a process with an ICO. In addition to describing ICO, higher-order processes can be used to describe non-Markovian processes, and higher-order process tomography has been experimentally implemented in this context[66–69].

Theory-independent demonstration

Although the DD techniques can detect the presence of an ICO, they require the assumption that quantum theory applies to the experiment. In 2019, this assumption was relaxed, creating a 'theory-independent' protocol by leveraging Bell's inequality[70]. The authors of ref. 70 considered a scenario wherein two states initially cannot violate a Bell inequality. They then imagined sending these two states into two different quantum switches, with entangled control qubits, as the respective target state (Fig. 2d). They argued, without using the quantum theory, that unless the order of operations inside the quantum switches is indefinite, the target systems cannot be used to violate a Bell inequality. This proposal was later adapted to a photonic setting[33], performing an experiment using two quantum switches sharing entangled path control qubits. In the experiment, the causally non-separable process was validated by the violation of a Bell inequality with a Bell parameter of $S_{\text{target}} = 2.55 \pm 0.08$, from an initially separable target state.

Semi-device-independent approaches

The techniques discussed thus far require trust in the experimental apparatus. A protocol that removes this assumption completely is said to be DI, whereas partially removing it results in a semi-DI protocol. In a semi-DI approach, one can use quantum mechanical descriptions of parts of the experimental devices while making no assumptions about the other parts (Fig. 2c). This is what is typically meant by semi-device independence in quantum-information scenarios such as Einstein–Podolsky–Rosen steering[71–73] and quantum cryptography[74]. Semi-DI approaches for causal witnesses were developed in refs. 75,76. For example, ref. 75 considered the quantum switch as a tripartite process in which Alice and Bob are the parties in the switch and Charlie is a third party who performs measurements after the switch. They considered various scenarios wherein not all three parties are completely trusted and showed how to derive semi-DI causal witnesses for each case.

Building on this proposal[75], another study[35] performed an experiment using a photonic quantum switch in which both parties inside the quantum switch performed measure-and-reprepare channels. This experiment allowed for two parties to be untrusted, where one of the trusted parties should be in the switch (Alice or Bob) and the other party (Charlie) was the measurements after the switch. The study was also notable in that it was the first experiment to equip both parties with such measure-and-reprepare channels.

Causal inequality and device-independent techniques

Bell's inequality is perhaps the best-known DI protocol[77–80]. Its violation has profound implications for our understanding of the nature of non-locality[81–83], telling us, irrespective of quantum theory,

that nature allows for non-local correlations. From a more mundane point of view, it can also be used as a tool to certify the presence of entanglement[84,85]. To maintain our analogy between ICO and entanglement certification, 'causal inequalities' take the place of Bell's inequality for ICO. These inequalities were first proposed in ref. 12 and concern the correlations between two parties. Making three assumptions: first, the parties operate in a fixed causal order; second, they can freely choose their measurement and third, they operate in closed laboratories, ref. 12 bounded the allowed correlations between the two parties if their order is predefined. By working in a completely DI framework, the authors of this work showed that these bounds must hold even if a new theory eventually supersedes the quantum theory. Thus, a loophole-free violation of such a causal inequality would definitively prove that processes can exist wherein there is no well-defined order between the events. They further showed that a quantum process, now known as the OCB process, exists that can exceed these correlations. Various follow-up studies have continued to analyse similar causal inequalities[41,42,86–90].

Although it is possible to write out a process matrix that violates a causal inequality, it is now not yet known how to experimentally realize such a process. For example, it is known that the quantum switch cannot be used to violate a causal inequality[13,54] and it has been suggested that any physically implementable process should be purifiable[57]. A purifiable process is one that can be described as a unitary process in some larger Hilbert space whenever A and B are unitary. The OCB and related processes are not purifiable[57]. Although the violation of causal inequalities could be simulated using post-selection[91,92], this approach would not allow one to make a DI conclusion about processes with ICO.

Nevertheless, the allure of causal inequalities continues to motivate researchers to find alternative approaches to device-independently certify ICO without using causal inequalities. For example, a recent proposal to do this using the quantum switch is based on a strategy in which the control system is entangled with an ancillary space-like-separated qubit[60,93]. This work (schematically presented in Fig. 2e) leverages tools from Bell's theorem and is somewhat inspired by Wigner's friend[94]. This highlights the possibility of transforming broader proofs of Bell non-locality into proofs of ICO using quantum switches and potentially other physically implementable processes. For example, moving beyond the Clauser–Horne–Shimony–Holt inequality, it has been proposed that Mermin's proof of non-locality using Greenberger–Horne–Zeilinger states could be tailored to ICO and provide an even stronger DI certification of ICO[61], without violating a causal inequality.

Applications exploiting ICO

In addition to its fundamental value, an ICO can also lead to advantages in quantum-information tasks. One can even establish resource theories for ICO[95], just as is done for phenomena such as entanglement[96]. Although ICO does not provide a universal improvement to all quantum algorithms or quantum circuits[97], there are many specific ICO-enhanced applications, which we will now review.

Promise problems

The first proposal to use an indefinite causal structure as a quantum resource was made for a channel discrimination task[98] and was later generalized[26,44,63,99,100]. In the channel discrimination task of ref. 98, two unknown unitary channels are promised to commute or anti-commute and the goal is to determine which relation they obey. When the channels are embedded in a causally ordered circuit, perfect discrimination between these two relations requires two queries to at least one of the channels. However, it was shown that a quantum superposition of two different causal orders with each channel being used only once could achieve perfect success. In 2015, ref. 10 used a quantum switch, with a path control system and a polarization target system, to distinguish commuting qubit gates from anti-commuting ones. This result was also implemented using the phase-stable Sagnac geometry[29].

The original problem[98] was later extended to the case involving N unitary gates in ref. 26, in a task often called a Fourier promise problem. The authors showed that an N-switch can distinguish between these $N!$ promises with each gate being queried only once, whereas the best causal algorithm at the time, through simulation of an N-switch using causally ordered circuits, calls the gates $O(N^2)$ times. However, this protocol also requires the dimension of the target system to grow as N. Furthermore, the advantage was later reassessed and a more efficient causal algorithm was proposed, showing that only $O(N\log(N))$ queries were required[101], reducing the advantage of the N-switch to $\log(N)$. Nevertheless, no evidence has so far invalidated the advantage of ICO in this problem. In any case, the experimental implementation of an N-gate Fourier promise problem is very demanding because it requires the dimensions of both the control and target systems to be at least $N!$. In 2021, ref. 44 addressed both of these challenges by constructing a so-called Hadamard promise problem for four gates. In this scenario, only a subset of the possible permutations of the four gates is used, thus the dimension of the control system could be much less than $N!$. In addition, the black-box unitaries could be chosen as qubit gates, allowing the use of polarization as the target system. The protocol was demonstrated with a photonic quantum switch in which a 4D path control and four polarization qubit gates were involved. Shortly after this, ref. 99 generalized these Hadamard promise problems to N gates, showing that a best causal quantum algorithm required $O(N\log(N))$ queries to the gates, whereas using the quantum N-switch only requires each gate to be used once.

Communication complexity

Communication complexity[102] is an important form of communication, in which several distributed participants collaborate to calculate a public function that depends on their private input strings. It is already well known that quantum resources can yield an exponential advantage in this task[103,104], and this is, therefore, a natural setting to look for ICO advantages. In 2014, ref. 105 found that in a three-party signalling game, the third party can perfectly determine the sum modulo 2 of the inputs of the other two parties. On the other hand, when using a causally-ordered process they can only succeed with a probability of at most 5/6. It was pointed out[106] that an ICO can provide similar advantages in the $(\log_2 3, 2)$ Hamming game. However, in both of these protocols, no general scaling advantage was proposed.

In 2016, ref. 16 found an exponential scaling advantage of ICO for the two-party exchange evaluation game. Here, only one-way communication is permitted and the inputs for each participant contain an n-bit string and a private Boolean function. With the help of ICO, only n qubits of communication are needed to achieve deterministic success, whereas for causally ordered strategies the required number of qubits of communication grows exponentially as $(2^n + n - 1)/2$. The experimental demonstration of this requires a two-party quantum switch acting on an n-qubit target system.

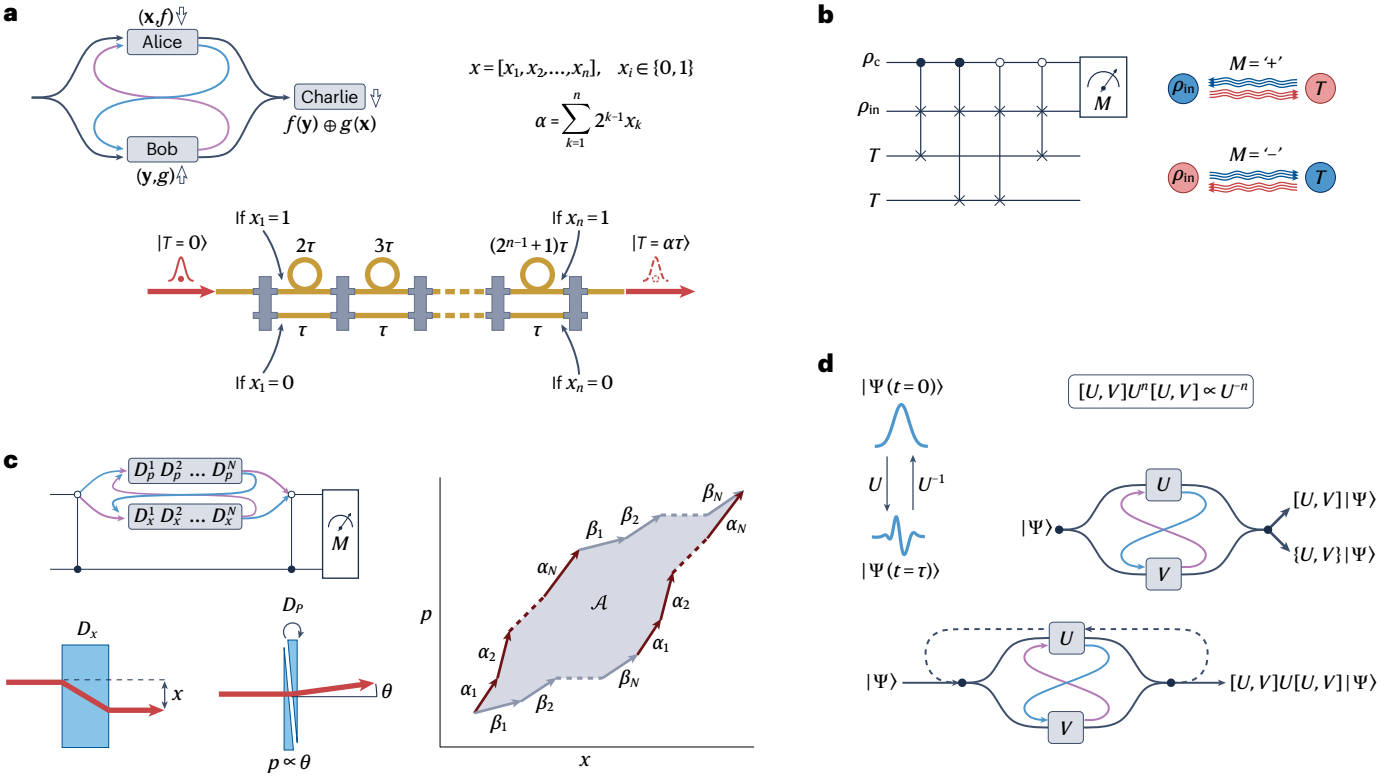

Fig. 3 | Experimental applications of indefinite causal order processes. **a**, The exponential communication advantage of ref. 16. Two parties, Alice and Bob, have Boolean functions f and g with input bit strings x and y, respectively. Charlie, the third party, must evaluate the logical XOR of outputs of Alice and Bob. In the realization of this advantage in ref. 17, the bit strings were encoded in unitary operations that the two parties implemented on the time degree of freedom of the photon, using the apparatus at the bottom of the panel. Dependent on the individual bit value x_k, the photon sees the short path (time delay τ) or the long path (time delay $(2^{k-1}+1)\tau$), such that the photon experiences an overall delay of $\alpha\tau$. α is unique for each bit string, as defined in the figure. These two operations are inserted in a propagation-direction controlled quantum switch (not pictured). **b**, Two thermalizing channels acting in a superposition of orders can bring a system out of thermal equilibrium. This was simulated using the above quantum circuit in refs. 47,48. Therein, ρ_c (ρ_{in}) is the control (target) system, and two bottom qubits are in thermal states T. When post-selecting on the measurement outcome '$M = +$' ('$M = -$') at the end of the circuit, heat flows from (to) the input system to (from) the thermal bath. **c**, In ref. 19, an indefinite causal order was used to demonstrate true super-Heisenberg sensing of up to eight independent phase-space displacements. These were realized using position D_x^i and momentum D_p^i displacements of an optical beam. D_x^i were generated by MgF_2 plates to displace the beam by x through polarization walk-off. D_p^i were implemented with wedge pairs to deflect the beam by an angle θ. The plot on the right represents the phase-space displacements implemented by the two parties in the quantum switch. α_i (β_i) are the displacements of the first (second) party, and $\mathcal{A}$ is the enclosed area, corresponding to the total geometric phase to be detected. **d**, In ref. 18, an indefinite causal order process was used to realize the time reversal of a quantum system. In the experiment, the free evolution U of a qubit system was superposed with a perturbed evolution V inside a quantum switch. This causes the system $|\Psi(t)\rangle$ to evolve backwards in time, independent of the initial state of the system, as well as its free and perturbed evolution. Panel **c** is adapted with permission from ref. 19, Springe Nature Ltd; panel **b** is adapted with permission from ref. 48, APS.

An experiment[17] implemented this approach with a target system up to $d = 2^{13}$ dimensions (Fig. 3a). Given the high dimensionality of the target system, this experiment revealed a scaling advantage, reducing the required communication by 65.2 ± 0.3% and 30.4 ± 0.6% when compared with any classical strategy and any causally ordered quantum strategy, respectively.

Quantum communication

In 2018, it was realized that it was possible to use the quantum switch to enhance communication rates through noisy channels. In a series of two papers[107,108], the authors considered communication through two copies of a noisy quantum channel. In general, if two noisy channels are combined in a fixed causal order, then the net result is a noisier channel; this is formalized in the 'bottleneck inequality'[109]. However, if the channels are combined with an ICO, the overall noise can actually decrease. This can be achieved for transmitting both classical[107] and quantum[108] bits. For certain noise models, even perfect communication can be made possible by the quantum switch[110]. Reference[28] reported the first experimental study of the transmission of classical information through two completely depolarizing channels. Other experimental studies of ICO-enhanced quantum communication followed[32,34]. These effects seem to contradict the standard quantum Shannon theory, which has led to generalizations of the Shannon theory that include 'superposition of trajectories'[111,112]. These results have since been generalized to communication through more than two noisy channels[113–115] and even to ICO-enhanced quantum state teleportation in the presence of noise[116].

Initial work attributed this effect to ICO, dubbing the effect 'causal activation'[107]. However, shortly after the initial proposals, it

was noted that coherence between a target and control system can also lead to noise cancellation[117,118], which is similar to error filtration[119]. In these proposals[117,118], a photon is placed in a superposition of different trajectories and those trajectories are routed through noisy channels in different manners, but in a fixed order. Although there are still discussions in the community regarding this effect, the general consensus is that the use of a noiseless control system allows one to partially or fully encode information in the control system, opening a side channel and thus avoiding the noise which only acts on the target space. References[32,120] have since studied different noise cancellation protocols experimentally. Moreover, similar noise cancellation effects have been proposed in the context of standard quantum computation, wherein correlations with ancillary systems are used to overcome noise in quantum computations[121–123]. Thus, to summarize, the ICO-based communication advantages are only present when comparing the switch with fixed-order processes without auxiliary systems.

Although noise reduction may be the most well-known application of ICO to quantum communication, ICO can also enhance the performance of other quantum communication tasks. Many of which have not yet been experimentally studied. In 2023, an ICO-based quantum key distribution (QKD) protocol was proposed[124], in which the directions of the key shared between Alice and Bob are superposed in a quantum switch. In this QKD protocol, the presence of eavesdroppers can be detected by only measuring the control system, thus saving a subset of keys that would be consumed during the public key comparison phase of standard QKD. ICO can also be used to realize the deterministic generation of multipartite entanglement[125] and even multipartite higher-dimensional entanglement distribution[126]. The core idea here is to replace multipartite gates with local single-qubit unitary gates applied in an ICO[127]. In 2023, further advantages of ICO for entanglement distillation were revealed[128]. In a three-step entanglement distillation protocol, the fidelity of the final entanglement or the success probability can be made higher when two distillation steps are embedded in a quantum switch.

Thermodynamics

ICO can also benefit quantum thermodynamics, in particular, in the construction of quantum refrigeration[46], quantum battery charging[129] and thermodynamic work extraction[130–132].

In 2020, ref. 46 discovered that a system can extract or release heat from two identical reservoirs that are placed in a quantum switch. An ICO refrigerator was then proposed by combining these ICO-assisted thermalization processes with two classical thermalization processes. The enhancement effect of ICO in work extraction was reported in terms of free energy[130] and ergotropy[131,132]. In 2021, ref. 129 showed that an ICO-enhanced unitary charging process could achieve full charging. This has been generalized to non-unitary charging protocols and was experimentally demonstrated using a photonic quantum switch[36]. Therein it was shown that ICO can boost the efficiency of a quantum-battery charging process and give rise to an anomalous effect whereby weaker chargers exhibit higher efficiency. In addition to enhancements based on the quantum switch, quantum thermodynamics with indefinite time directions has also been investigated[133,134].

ICO-enhanced thermodynamics studies the heat or workflow between the reservoirs when the reservoirs are placed in the quantum switch. In 2022, ref. 20 reported a photonic implementation of ICO-induced quantum refrigeration, in which a photonic polarization qubit serves to interact with two reservoirs in an ICO. The reservoirs were achieved by constructing thermal channels to simulate their interactions with the working system. The temperature and energy change were defined as changes in the population of photons in the horizontal and vertical polarization states[135,136].

ICO-enhanced quantum refrigeration was also investigated[48] in an NMR system (Fig. 3b). In this work, three nuclear spins acted as a qubit and two reservoirs, whereas a fourth spin was used as a control system. The equivalent four-qubit unitary quantum circuit proposed in ref. 46 was implemented. A similar approach was implemented on an IBM cloud quantum computer[47]. See also ref. 137 for a summary of ICO-enhanced quantum refrigeration.

It was pointed out in ref. 138 that a particular causally ordered non-Markovian process can give an enhancement that is similar to ICO-based proposals[130,132]. As discussed before, the issue is how the control system interacts with the protocol. In some scenarios, coherence between the control and target systems can lead to very similar advantages even if all the operations are applied in a definite causal order. Analogous effects have been investigated in ICO-enhanced quantum communication[139–141] and the results revealed that an increase in information capacity consumes a thermodynamic resource: the free energy of coherence associated with the control system of the quantum switch.

Quantum metrology

Several studies have suggested that ICO can also enhance quantum metrology. In 2019, ref. 142 showed that ICO can enhance the precision in identifying the properties of a depolarizing channel. ICO was further proposed to be used in noisy metrology tasks in which other noisy channels are involved in qubit unitary channel estimation games[143,144]. In general, complex measurements are needed to achieve the optimal estimation strategy. With ICO, however, one can achieve near-optimal precision with a simple projective measurement on the control qubit. This was demonstrated in a photonic experiment in which a phase flip channel and a depolarizing channel were used[37]. However, it can be difficult to claim a real advantage from ICO, just as in the case of enhanced quantum communication through noisy channels. To make such general claims, one must compare the ICO strategy with all possible fixed-order strategies. There have been several attempts to provide a general framework for this comparison[145–147]. Notably, by extending the framework of ref. 146, it was found that for the tasks of single-parameter estimation in a discrete variable system, it is possible to find a strategy with a definite causal order that outperforms the quantum switch[147]. Moreover, ref. 145 proved that, within discrete-variable systems, ICO can only achieve the Heisenberg scaling, which is the fundamental limit of the precision in quantum metrology. However, these frameworks have not yet been extended to multiparameter quantum estimation, such as the multiparameter proposal of ref. 148. In the case of continuous-variable systems, it is possible to achieve provable metrological advantages from ICO[149].

Achieving scaling beyond the Heisenberg limit has been a long-standing goal of quantum metrology. An ICO-enhanced metrology task surpassing the Heisenberg limit was proposed[149] in 2020. The authors proved that quantum switch can help to achieve super-Heisenberg scaling when estimating the product of continuous-variable position and momentum displacements of a harmonic oscillator. Although the use of indefinite causal structure for continuous-variable systems has been theoretically analysed[150], its experimental implementation requires delicate quantum engineering.

In 2023, ref. 19 realized super-Heisenberg scaling in a photonic system (Fig. 3c). In this experiment, the position x and momentum p displacements were defined in the transverse direction of a single

photon and their product was the geometric phase in the *xp*-phase space. Approximately 18.6 μm of position displacement and approximately 2.8×10^{-4} rad of momentum displacement were prepared to ensure a tiny geometric phase (0.042). With at most $N = 8$ pairs of displacements used in the quantum switch, the experiment observed a root-mean-square error of the geometric phase with a scaling $\propto 1/cN^2$ ($c \approx 30.65$), showing significant evidence of the super-Heisenberg limit.

Other applications

ICO can also benefit the investigation of other phenomena in the foundations of quantum mechanics. Here, we briefly summarize various proposals on this topic.

In 2023, ref. 151 demonstrated that ICO could suppress the decoherence effect of reservoirs on a quantum system, thus reducing the decay of its quantumness, including coherence, temporal steering, entanglement and Bell non-locality. Ref. 152 showed how to use a quantum switch to efficiently estimate the incompatibility of quantum measurements and further applied this protocol to cluster quantum observables with an unsupervised algorithm. The quantum switch can help to close the clumsiness loophole in the Leggett–Garg test, thus providing a loophole-free protocol to examine the boundary between classical worlds and quantum ones[153]. In 2022, ref. 154 proposed the teleportation of a quantum causal structure by simply teleporting all of its inputs and outputs. ICO was also proven to be advantageous in channel discrimination tasks in which two non-signalling bipartite channels[98] or even multiple copies of arbitrary unitary channels[63,100] were involved. None of the aforementioned protocols have been experimentally implemented.

Another example that has been experimentally studied is universal quantum rewinding. The goal of quantum rewinding is to reset a quantum system subjected to an unknown evolution to its state at an earlier time. In 2019, ref. 155 showed how to implement the exact inverse of a unitary operation with a failure probability that decays exponentially in the copies of operation used. Using semi-definite programming methods, it was also proved that ICO could achieve a higher probability of success than circuits based on parallelized and adaptive strategies under certain constraints, and in ref. 156, a similar result for unitary transposition was demonstrated. By using rigorous computer-assisted proof methods, ICO has also been shown to give an advantage in deterministic but non-exact unitary inversion[157]. It is worth nothing that a quantum circuit for exact and deterministic inversion of a qubit unitary, using four copies of the gate, was found[158]. This does not contradict the aforementioned advantages, as they concern fewer gate uses and, in the case of ref. 157, also apply to higher dimensions. In 2023, a more practical rewinding protocol was presented[159] and experimentally demonstrated[18]. The core idea is to utilize the non-commutativity of an unknown target process and an auxiliary process, which makes it well suited for the quantum switch, which can distinguish commuting from anti-commuting gates. Moreover, the probability of success can be boosted arbitrarily close to one by cascading quantum switches (Fig. 3d). In the experiment, electro-optical devices and time synchronization techniques were used to quickly route photons through the quantum switch. The experiment observed an average reversal fidelity of more than 95%.

Loopholes and criticisms of current experimental demonstrations

Although the field of experimental ICO has been extremely successful, there have been several noteworthy criticisms of the experimental implementations. Nevertheless, experimental work has continued to be defended by strong theoretical arguments from many in the ICO community[160–162]. Here, we briefly summarize this discussion from an experimental point of view.

The first criticism to appear in the literature can be considered as a 'multiple use problem'. It states that since two paths traverse each optic, experimental quantum switches (Fig. 4a) are equivalent to an 'unfolded switch'[2] (Fig. 4b). Thus, quantum switch experiments use each gate twice. One can attempt to simply count the number of times the photon traverses each optic[10,26]. However, as we discuss in Box 2, counting gate uses in experimental settings is quite subtle, and most attempts to operationally count the gate uses support the point of view that the experiments only use each gate once.

The other major criticism can be termed the 'multiple event problem'[163–165], illustrated in Fig. 4c. It can be summarized as follows. In the experiment with two gates, each experiment consists of two time steps. At time t_1, the photon is in a superposition of traversing gate 1 and gate 2, and at time t_2 it is in a superposition of traversing gate 2 and gate 1. This situation corresponds to four different space-time events. However, just as a photon can be in a superposition of spatial modes, a photon can also be in a superposition of temporal modes. In fact, photons are always in some form of a wave packet with a temporal extent[166] (Fig. 4d, top). When this delocalized particle passes some device, it seems more natural, to think of time-delocalized events. In other words, the photon traverses the device in a superposition of times. If this is the case for a photon in an extended wavefunction (Fig. 4d, top), it also applies to a photon in a superposition of discrete times (as sketched in the bottom of Fig. 4d). The full formal argument is presented in ref. 160. From an experimental point of view, this 'temporal uncertainty' was exploited using photons with a coherence time longer than the propagation time between the two gates[15]. Thus, quantum mechanically, in this work, it is impossible to define four unambiguous space-time events. A different approach to overcome this critique has also been proposed in ref. 167, in which the spontaneous decay from two excited atoms could be used to implement the quantum switch in a table-top setting with only two space-time events.

Despite these arguments, some researchers maintain that photonic experiments performed to-date do not implement a true ICO[163]. In ref. 165, it was argued that because the photon is in a superposition of different space-time locations, the gates must be applied not only on the photon itself but also on the vacuum system; this admits an alternative 'fine-grained' causal order, which does not have an ICO. A very similar fine-graining argument was presented in ref. 164. Another common theme among critiques of experimental implementations is that perhaps the gravitational quantum switch is required to implement a true ICO[163–165].

The gravitational quantum switch was proposed for realizing an ICO by creating a superposition of massive objects[70]. Consider two events, A and B, placed between a massive object that is in a superposition being to the left of B (Fig. 4e, bottom) or to the right of A (Fig. 4e, top). Owing to gravitational time dilation, time passes more slowly closer to the massive object, so in one case event B will occur first (Fig. 4e, top), whereas in the other case, event A will occur first (Fig. 4e, bottom). This superposition of masses can thus be used to realize a quantum switch. The gravitational quantum switch and the photonic quantum switch were shown to be completely equivalent in terms of the causal order between the events[161].

Given the discussion surrounding experiments, device-independent and theory-independent techniques to demonstrate ICO

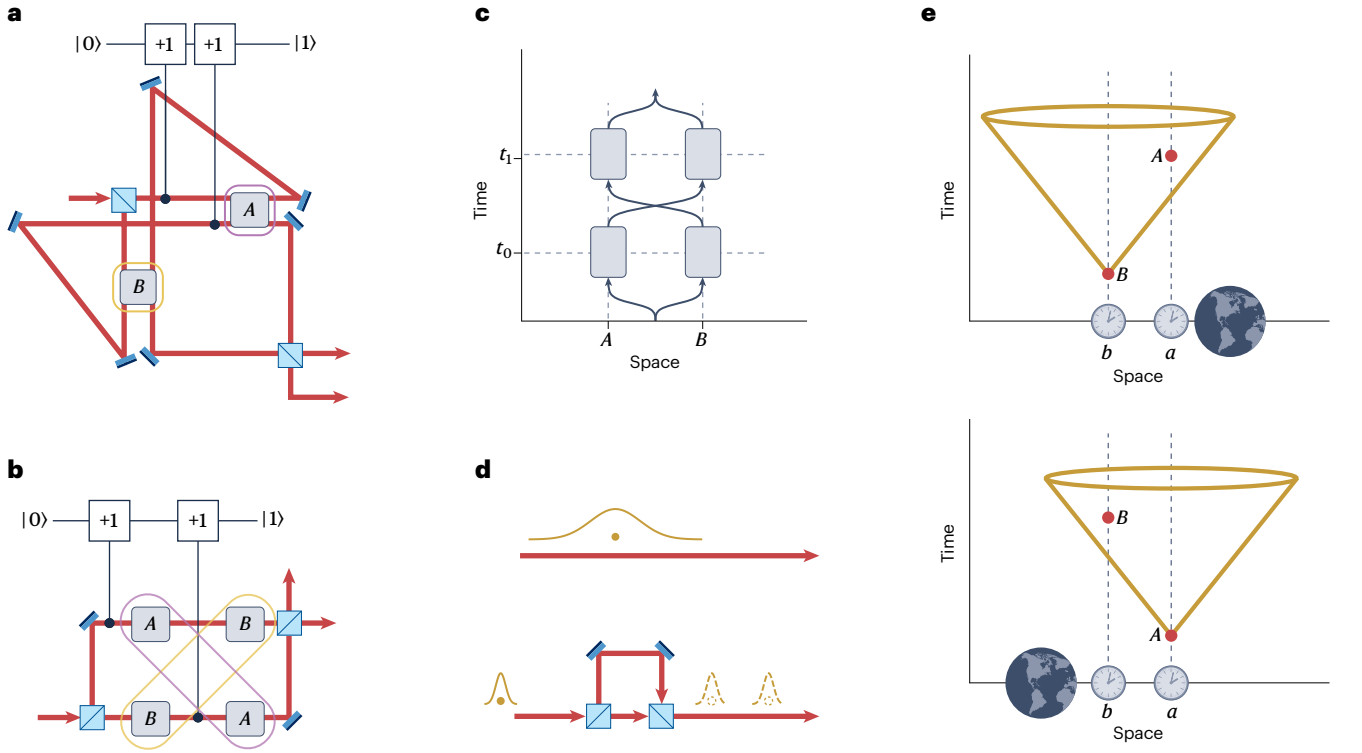

Fig. 4 | Experimental loopholes. a, The quantum switch with a path control system, operations *A* and *B*, and a hypothetical counter system (the upper system initialized in $|0\rangle$) that is used to count the number of gate uses. After the experiment is run, the counter system is left in the state $|1\rangle$, indicating that gate *A* has only been used once. **b**, The so-called unfolded switch. Using two identical copies of the optical elements used to implement gates *A* and *B*, one can use a Mach–Zehnder geometry to build a device that produces the same statistics as the quantum switch. Even the upper counter system will behave the same. However, in this device, one cannot associate non-overlapping spatial regions with gate *A* or *B*. **c**, Space-time diagram of the experimentally implemented quantum switch. At time t_0, the photon is in a superposition of being at both gates *A* and *B*. At time t_1, it is again in a superposition of both locations, but swapped with respect to t_0. Even though the 'counter-argument' can be used to conclude that the photon only interacts with each gate once, the four distinct space-time events have led some to conclude that the quantum switch does not have a genuine indefinite causal order. **d**, Time-delocalized events. In practice, a photon can never be perfectly localized in time, making it difficult to define events in experimental implementations of the quantum switch. Top: a photon must exist with some extended wave packet, implying that it traverses an optical element in a superposition of different times. Bottom: using an unbalanced interferometer, a photon is placed in superposition of two time bins and thus travels in a superposition of being centred at two distinct times. **e**, The gravitational quantum switch from ref. 70. By placing a massive object in a quantum superposition, one can implement the quantum switch. In the branch of the superposition with the massive object on the left (right), the photon experiences event *A* (*B*) at spatial location *a* (*b*) before event *B* (*A*) at spatial location *b* (*a*). Panel **e** is adapted with permission from ref. 70, CC BY 4.0.

are clearly needed and progress towards this goal is being made both on the experimental and theoretical fronts. Indeed, a proposal for a device-independent verification[60] makes an important step in this direction. However, the identification of all experimental loopholes and finding a way to close them experimentally is still a work in progress. One of the most notable loopholes is that both superposed parties act in a 'closed laboratory'[12]. This assumption is used to exclude trivial communication between the two parties; in other words, the third assumption in the section on 'Causal inequality and device-independent techniques' essentially constrains the signalling direction. That is, one-way signalling is allowed, whereas bidirectional signalling is forbidden. For a fixed causal order, if Alice (Bob) acts first, then input of Bob (Alice) can be perfectly correlated with the output of Alice (Bob), but there can be no correlations between the input of Alice and the output of Bob. In a standard Bell-like scenario, this situation could be enforced in a space-like way by separating the two parties. However, in the quantum switch, this is not possible as the two parties must exchange a quantum system. Instead, one could attempt to enforce such a situation by only allowing each party to act exactly once. However, given the difficulty in even defining what it means for a party to act (or a gate to be applied), it is not clear how to verify this assumption experimentally, let alone in a DI way.

Outlook

ICO is an exciting research topic that lies firmly at the intersection of quantum foundations and quantum information[168]. Various innovative implementations of ICO processes have been proposed, motivated by foundational questions and new quantum applications. In this Review, we have separated the experimental research into two parts: work attempting to verify ICO and work using ICO for applications. In both cases, the amount of theoretical research and number of proposals outweigh the experimental tests and implementations, leaving an ample playground for experimentalists.

On the one side, in order for the quantum switch to prove truly useful for applications, it should be scaled up. Depending on the

Box 2 | Counting gate uses

For many applications, the advantage of the quantum switch is that they require fewer gate uses than traditional quantum circuits. It is, therefore, important to define what is meant by a gate use, which is non-trivial when using essentially classical resources (such as a wave plate, laser or radiofrequency pulse) to coherently manipulate a quantum system. For example, in a trapped-ion quantum computer, a single laser pulse can simultaneously manipulate each ion in the trap. Should this be considered as: one gate use as a single pulse was used; one gate use for each ion in the trap; or many more gate uses, as not all of the light is absorbed by the ions, and in principle the same pulse could manipulate many more ions?

Using wave plates to manipulate photonic qubits, as is done in photonic quantum switch experiments, is a very similar situation. In principle, one could send a nearly infinite number of orthogonal optical modes through a given optical element. To take a more concrete experimental perspective, one could ask how much energy flows through each optical element. The energy transmitted through a given area is given by the optical power integrated over the experimental time[166]. This power is proportional to the photon occupation number and does not depend on the mode shape or even the number of modes. Thus, when a single photon is placed in a superposition of any number of modes (be they spatial modes, spectral modes or transverse electrical modes), the energy traversing the gate is the same. From this point of view, only one photon traverses the gate per experimental run.

Phrasing this argument in an operational quantum manner, one can imagine using an ancillary system to coherently count how many times the photon passes through the gate (Fig. 4a). As the energy is proportional to the photon flux, these two arguments lead to qualitatively similar results. In particular, imagine a qudit counter system in state $|0\rangle$ that interacts with the switch photon via two 'controlled-plus' gates. In this interaction if a particle traverses the control path, then the state of the qudit system evolves as $|j\rangle \rightarrow |(j+1) \bmod d\rangle$, in which d is the dimension of the system. Therefore, with this hypothetical situation, the auxiliary system counts how many times the photon passes each gate. A straightforward calculation shows that after the experiment, the qudit is left in the state $|1\rangle$, indicating that the gate has only been used once. One could also use a counting system in the unfolded switch (Fig. 4b), but then one cannot associate a single non-overlapping spatial region to either gate; that is, the spatial regions (encircled yellow and violet regions in Fig. 4b) must cross.

Another approach theoretically analysed a situation wherein an additional quantum system (an atom in a cavity) is used to implement a gate. As this requires the atom to transition between different energy states, it allows to associate an energy cost to each gate use. The energy cost of implementing quantum gates can be calculated both in the standard switch and in the unfolded switch. It was shown that the unfolded configuration requires more energy than the standard switch[162].

application, the dimensions of the target system, the control system or both must be increased. Although the target scaling has been demonstrated with a 2^{13}-dimensional system[17], scaling up the control system remains a challenge. In all current experimental implementations, each additional superposed causal order requires the dimension of the control system to increase by 1. As the complete N-switch superposes $N!$ orders, this means that $N!$ modes must traverse each optical element. This difficulty has limited the number of experimentally superposed causal orders to four[44]. To overcome this experimental challenge, one could take two approaches. First, one could take the brute force approach and simply use a control DoF, which may be easier to engineer. To this end, the approach of using a time-bin control may have some advantages. Although experimental demonstrations have thus far been limited to a two-gates system[31], an N-gate switch proposal has been worked out[39]. This does not, however, deal with the scaling challenge: in fact, that proposal requires N^N time bins to implement the full quantum N-switch. Instead, a scalable (albeit more difficult) approach could require a multiqubit register encoded in a different physical system to encode the control. In this case, a multiqubit state would select the order to be implemented, and thus the physical resources could scale much more favourably in terms of the number of orders to be superposed. However, if the target system is encoded in a photon, single-photon-level nonlinearities are needed, which are still challenging for photonic experiments. Nevertheless, this approach may be a promising new path for the next generation of ICO experiments.

We discussed various criticisms of experimental implementations of the quantum switch. When it comes to applications, if a process that simulates an ICO or is inspired by an ICO can outperform standard techniques, this could still lead to some practical advantages, as in ICO-inspired noise-cancellation proposals[121–123]. However, these criticisms are of more concern when one claims that the advantage can only be achieved with an ICO, as it may obfuscate the underlying physics. These issues are, of course, of utmost importance for work verifying ICO. In this respect, we believe that the push to verify ICO using DI techniques is necessary. To this end, new theory has led to semi-DI experimental tests of ICO[33,35]. Moreover, proposals are opening the door for other types of experimental device-independent tests of ICO[60]. Of course, any future experiments making such bold claims will need to be carefully examined for loopholes, with the closed laboratory assumption[12] likely being the most important. Although a better theoretical understanding is still required, the current situation is not unlike the use of inequalities of Bell to verify entanglement before the seminal set of 2015 experiments[169–171]. Thus, we believe that there is much exciting and ground-breaking work that remains to be done in the field of ICO.

Published online: 19 July 2024

References

1. Ried, K. et al. A quantum advantage for inferring causal structure. *Nat. Phys.* **11**, 414–420 (2015).
2. Maclean, J.-P. W., Ried, K., Spekkens, R. W. & Resch, K. J. Quantum-coherent mixtures of causal relations. *Nat. Commun.* **8**, 15149 (2017).
3. Carvacho, G. et al. Experimental violation of local causality in a quantum network. *Nat. Commun.* **8**, 14775 (2017).
4. Carvacho, G., Chaves, R. & Sciarrino, F. Perspective on experimental quantum causality. *Europhys. Lett.* **125**, 30001 (2019).
5. Chiribella, G. & Ebler, D. Quantum speedup in the identification of cause–effect relations. *Nat. Commun.* **10**, 1472 (2019).

6. Tavakoli, A., Pozas-Kerstjens, A., Luo, M.-X. & Renou, M.-O. Bell nonlocality in networks. *Rep. Prog. Phys.* **85**, 056001 (2022).
7. Hardy, L. Towards quantum gravity: a framework for probabilistic theories with non-fixed causal structure. *J. Phys. A Math. Gen.* **40**, 3081–3099 (2007).
8. Hardy, L. in *Quantum Reality, Relativistic Causality, and Closing the Epistemic Circle* 379–401 (Springer, 2009).
9. Chiribella, G., D'Ariano, G. M., Perinotti, P. & Valiron, B. Quantum computations without definite causal structure. *Phys. Rev. A* **88**, 022318 (2013).
The paper in which the quantum switch was first proposed. It showed that the quantum switch could be used to accomplish tasks that cannot be done in the quantum circuit model.
10. Procopio, L. M. et al. Experimental superposition of orders of quantum gates. *Nat. Commun.* **6**, 7913 (2015).
The first experiment to implement the quantum switch, demonstrating the advantage of indefinite causal order by playing a promise problem.
11. Colnaghi, T., D'Ariano, G. M., Facchini, S. & Perinotti, P. Quantum computation with programmable connections between gates. *Phys. Lett. A* **376**, 2940–2943 (2012).
12. Oreshkov, O., Costa, F. & Brukner, Č. Quantum correlations with no causal order. *Nat. Commun.* **3**, 1092 (2012).
The theoretical paper which first defined the notion of causal non-separability.
13. Araújo, M. et al. Witnessing causal nonseparability. *N. J. Phys.* **17**, 102001 (2015).
14. Rubino, G. et al. Experimental verification of an indefinite causal order. *Sci. Adv.* **3**, e1602589 (2017).
The first experimental measurement of a causal witness, which also represents the first time that the causal non-separability of a process was explicitly measured.
15. Goswami, K. et al. Indefinite causal order in a quantum switch. *Phys. Rev. Lett.* **121**, 090503 (2018).
16. Guérin, P. A., Feix, A., Araújo, M. & Brukner, Č. Exponential communication complexity advantage from quantum superposition of the direction of communication. *Phys. Rev. Lett.* **117**, 100502 (2016).
17. Wei, K. et al. Experimental quantum switching for exponentially superior quantum communication complexity. *Phys. Rev. Lett.* **122**, 120504 (2019).
An application-based experiment showing the exponential advantage that can be obtained with the quantum switch at a communication complexity task.
18. Schiansky, P. et al. Demonstration of universal time-reversal for qubit processes. *Optica* **10**, 200 (2023).
19. Yin, P. et al. Experimental super-Heisenberg quantum metrology with indefinite gate order. *Nat. Phys.* **19**, 1–6 (2023).
An experiment showing that an indefinite causal order can be used to obtain super-Heisenberg scaling in quantum metrology.
20. Cao, H. et al. Quantum simulation of indefinite causal order induced quantum refrigeration. *Phys. Rev. Res.* **4**, L032029 (2022).
21. Goswami, K. & Romero, J. Experiments on quantum causality. *AVS Quantum Sci.* **2**, 037101 (2020).
22. Brukner, Č. Quantum causality. *Nat. Phys.* **10**, 259–263 (2014).
23. Andersson, E., Bergou, J. & Jex, I. Comparison of unitary transforms using Franson interferometry. *J. Mod. Opt.* **52**, 1485–1494 (2005).
24. Zhou, X.-Q. et al. Adding control to arbitrary unknown quantum operations. *Nat. Commun.* **2**, 413 (2011).
25. Araújo, M., Feix, A., Costa, F. & Brukner, Č. Quantum circuits cannot control unknown operations. *N. J. Phys.* **16**, 093026 (2014).
26. Araújo, M., Costa, F. & Brukner, Č. Computational advantage from quantum-controlled ordering of gates. *Phys. Rev. Lett.* **113**, 250402 (2014).
27. Friis, N., Dunjko, V., Dür, W. & Briegel, H. J. Implementing quantum control for unknown subroutines. *Phys. Rev. A* **89**, 030303 (2014).
28. Goswami, K., Cao, Y., Paz-Silva, G. A., Romero, J. & White, A. G. Increasing communication capacity via superposition of order. *Phys. Rev. Res.* **2**, 033292 (2020).
29. Strömberg, T., Schiansky, P., Peterson, R. W., Quintino, M. T. & Walther, P. Demonstration of a quantum switch in a Sagnac configuration. *Phys. Rev. Lett.* **131**, 060803 (2023).
30. Liu, W.-Q. et al. Experimentally demonstrating indefinite causal order algorithms to solve the generalized Deutsch's problem. Preprint at https://arxiv.org/abs/2305.05416 (2023).
31. Antesberger, M., Quintino, M. T., Walther, P. & Rozema, L. A. Higher-order process matrix tomography of a passively-stable quantum switch. *PRX Quantum* **5**, 010325 (2024).
32. Rubino, G. et al. Experimental quantum communication enhancement by superposing trajectories. *Phys. Rev. Res.* **3**, 013093 (2021).
33. Rubino, G. et al. Experimental entanglement of temporal order. *Quantum* **6**, 621 (2022).
34. Guo, Y. et al. Experimental transmission of quantum information using a superposition of causal orders. *Phys. Rev. Lett.* **124**, 030502 (2020).
35. Cao, H. et al. Semi-device-independent certification of indefinite causal order in a photonic quantum switch. *Optica* **10**, 561 (2023).
An experiment taking steps to verify indefinite causal order going beyond the device-dependent framework, which is also notable in that both parties in the quantum switch were given non-unitary measure-and-reprepare channels.
36. Zhu, G., Chen, Y., Hasegawa, Y. & Xue, P. Charging quantum batteries via indefinite causal order: theory and experiment. *Phys. Rev. Lett.* **131**, 240401 (2023).
An experiment showing that indefinite causal order can boost the amount of energy charged and the thermal efficiency of quantum battery, showcasing the versatility of such processes.
37. An, M. et al. Noisy quantum parameter estimation with indefinite causal order. *Phys. Rev. A* **109**, 012603 (2024).
38. Reed, M. & Simon, B. *Methods of Modern Mathematical Physics: Functional Analysis* Vol. 1 (Gulf Professional Publishing, 1980).
39. Rambo, T. M., Altepeter, J. B., Kumar, P. & D'Ariano, G. M. Functional quantum computing: an optical approach. *Phys. Rev. A* **93**, 052321 (2016).
40. Dong, Q., Quintino, M. T., Soeda, A. & Murao, M. The quantum switch is uniquely defined by its action on unitary operations. *Quantum* **7**, 1169 (2023).
41. Abbott, A. A., Giarmatzi, C., Costa, F. & Branciard, C. Multipartite causal correlations: polytopes and inequalities. *Phys. Rev. A* **94**, 032131 (2016).
42. Abbott, A. A., Wechs, J., Costa, F. & Branciard, C. Genuinely multipartite noncausality. *Quantum* **1**, 39 (2017).
43. Wechs, J., Abbott, A. A. & Branciard, C. On the definition and characterisation of multipartite causal (non)separability. *N. J. Phys.* **21**, 013027 (2019).
44. Taddei, M. M. et al. Computational advantage from the quantum superposition of multiple temporal orders of photonic gates. *PRX Quantum* **2**, 010320 (2021).
45. Cariñe, J. et al. Multi-core fiber integrated multi-port beam splitters for quantum information processing. *Optica* **7**, 542 (2020).
46. Felce, D. & Vedral, V. Quantum refrigeration with indefinite causal order. *Phys. Rev. Lett.* **125**, 070603 (2020).
47. Felce, D., Vedral, V. & Tennie, F. Refrigeration with indefinite causal orders on a cloud quantum computer. Preprint at https://arxiv.org/abs/2107.12413 (2021).
48. Nie, X. et al. Experimental realization of a quantum refrigerator driven by indefinite causal orders. *Phys. Rev. Lett.* **129**, 100603 (2022).
49. Chiribella, G. & Liu, Z. Quantum operations with indefinite time direction. *Commun. Phys.* **5**, 190 (2022).
50. Mendl, C. B. & Wolf, M. M. Unital quantum channels — convex structure and revivals of Birkhoff's theorem. *Commun. Math. Phys.* **289**, 1057–1086 (2009).
51. Strömberg, T. et al. Experimental superposition of a quantum evolution with its time reverse. *Phys. Rev. Res.* **6**, 023071 (2024).
52. Guo, Y. et al. Experimental demonstration of input–output indefiniteness in a single quantum device. *Phys. Rev. Lett.* **132**, 160201 (2024).
53. Liu, Z., Yang, M. & Chiribella, G. Quantum communication through devices with indefinite input–output direction. *N. J. Phys.* **25**, 043017 (2023).
54. Purves, T. & Short, A. J. Quantum theory cannot violate a causal inequality. *Phys. Rev. Lett.* **127**, 110402 (2021).
55. Baumeler, Ä., Feix, A. & Wolf, S. Maximal incompatibility of locally classical behavior and global causal order in multiparty scenarios. *Phys. Rev. A* **90**, 042106 (2014).
56. Baumeler, Ä. & Wolf, S. The space of logically consistent classical processes without causal order. *N. J. Phys.* **18**, 013036 (2016).
57. Araújo, M., Feix, A., Navascués, M. & Brukner, Č. A purification postulate for quantum mechanics with indefinite causal order. *Quantum* **1**, 10 (2017).
58. Tselentis, E.-E. & Baumeler, ń. Admissible causal structures and correlations. *PRX Quantum* **4**, 040307 (2023).
59. Vanrietvelde, A., Ormrod, N., Kristjánsson, H. & Barrett, J. Consistent circuits for indefinite causal order. Preprint at https://arxiv.org/abs/2206.10042 (2022).
60. van der Lugt, T., Barrett, J. & Chiribella, G. Device-independent certification of indefinite causal order in the quantum switch. *Nat. Commun.* **14**, 5811 (2023).
A proposal for a device-independent verification of indefinite causal order that can be realized with the quantum switch; this proposal has yet to be experimentally implemented.
61. van der Lugt, T. & Ormrod, N. Possibilistic and maximal indefinite causal order in the quantum switch. Preprint at https://arxiv.org/abs/2311.00557 (2023).
62. Branciard, C. Witnesses of causal nonseparability: an introduction and a few case studies. *Sci. Rep.* **6**, 26018 (2016).
63. Bavaresco, J., Murao, M. & Quintino, M. T. Strict hierarchy between parallel, sequential, and indefinite-causal-order strategies for channel discrimination. *Phys. Rev. Lett.* **127**, 200504 (2021).
64. Svetlichny, G. Distinguishing three-body from two-body nonseparability by a Bell-type inequality. *Phys. Rev. D* **35**, 3066 (1987).
65. Seevinck, M. & Svetlichny, G. Bell-type inequalities for partial separability in *n*-particle systems and quantum mechanical violations. *Phys. Rev. Lett.* **89**, 060401 (2002).
66. Giarmatzi, C. et al. Multi-time quantum process tomography of a superconducting qubit. Preprint at https://arxiv.org/abs/2308.00750 (2023).
67. White, G. A. L., Hill, C. D., Pollock, F. A., Hollenberg, L. C. L. & Modi, K. Demonstration of non-Markovian process characterisation and control on a quantum processor. *Nat. Commun.* **11**, 6301 (2020).
68. White, G. A. L., Pollock, F. A., Hollenberg, L. C. L., Hill, C. D. & Modi, K. From many-body to many-time physics. Preprint at https://arxiv.org/abs/2107.13934 (2021).
69. Guo, Y. et al. Experimental demonstration of instrument-specific quantum memory effects and non-Markovian process recovery for common-cause processes. *Phys. Rev. Lett.* **126**, 230401 (2021).
70. Zych, M., Costa, F., Pikovski, I. & Brukner, Č. Bell's theorem for temporal order. *Nat. Commun.* **10**, 3772 (2019).
71. Wiseman, H. M., Jones, S. J. & Doherty, A. C. Steering, entanglement, nonlocality, and the Einstein–Podolsky–Rosen paradox. *Phys. Rev. Lett.* **98**, 140402 (2007).
72. Uola, R., Moroder, T. & Gühne, O. Joint measurability of generalized measurements implies classicality. *Phys. Rev. Lett.* **113**, 160403 (2014).

73. Quintino, M. T., Vértesi, T. & Brunner, N. Joint measurability, Einstein–Podolsky–Rosen steering, and Bell nonlocality. *Phys. Rev. Lett.* **113**, 160402 (2014).
74. Branciard, C., Cavalcanti, E. G., Walborn, S. P., Scarani, V. & Wiseman, H. M. One-sided device-independent quantum key distribution: security, feasibility, and the connection with steering. *Phys. Rev. A* **85**, 010301 (2012).
75. Bavaresco, J., Araújo, M., Brukner, Č. & Quintino, M. T. Semi-device-independent certification of indefinite causal order. *Quantum* **3**, 176 (2019).
76. Dourdent, H., Abbott, A. A., Brunner, N., Šupić, I. & Branciard, C. Semi-device-independent certification of causal nonseparability with trusted quantum inputs. *Phys. Rev. Lett.* **129**, 090402 (2022).
77. Aspect, A. Bell's inequality test: more ideal than ever. *Nature* **398**, 189–190 (1999).
78. Clauser, J. F., Horne, M. A., Shimony, A. & Holt, R. A. Proposed experiment to test local hidden-variable theories. *Phys. Rev. Lett.* **23**, 880 (1969).
79. Bell, J. S. On the Einstein–Podolsky–Rosen paradox. *Phys. Phys. Fiz.* **1**, 195 (1964).
80. Bell, J. S. On the problem of hidden variables in quantum mechanics. *Rev. Mod. Phys.* **38**, 447 (1966).
81. Weihs, G., Jennewein, T., Simon, C., Weinfurter, H. & Zeilinger, A. Violation of Bell's inequality under strict Einstein locality conditions. *Phys. Rev. Lett.* **81**, 5039 (1998).
82. Aspect, A., Grangier, P. & Roger, G. Experimental tests of realistic local theories via Bell's theorem. *Phys. Rev. Lett.* **47**, 460 (1981).
83. Freedman, S. J. & Clauser, J. F. Experimental test of local hidden-variable theories. *Phys. Rev. Lett.* **28**, 938 (1972).
84. Tóth, G. & Gühne, O. Detecting genuine multipartite entanglement with two local measurements. *Phys. Rev. Lett.* **94**, 060501 (2005).
85. Gühne, O., Lu, C.-Y., Gao, W.-B. & Pan, J.-W. Toolbox for entanglement detection and fidelity estimation. *Phys. Rev. A* **76**, 030305 (2007).
86. Oreshkov, O. & Giarmatzi, C. Causal and causally separable processes. *N. J. Phys.* **18**, 093020 (2016).
87. Brukner, Č. Bounding quantum correlations with indefinite causal order. *N. J. Phys.* **17**, 083034 (2015).
88. Branciard, C., Araújo, M., Feix, A., Costa, F. & Brukner, Č. The simplest causal inequalities and their violation. *N. J. Phys.* **18**, 013008 (2016).
89. Miklin, N., Abbott, A. A., Branciard, C., Chaves, R. & Budroni, C. The entropic approach to causal correlations. *N. J. Phys.* **19**, 113041 (2017).
90. Wechs, J., Branciard, C. & Oreshkov, O. Existence of processes violating causal inequalities on time-delocalised subsystems. *Nat. Commun.* **14**, 1471 (2023).
91. Silva, R. et al. Connecting processes with indefinite causal order and multi-time quantum states. *N. J. Phys.* **19**, 103022 (2017).
92. Dimić, A., Milivojević, M., Gočanin, D., Móller, N. S. & Brukner, Č. Simulating indefinite causal order with Rindler observers. *Front. Phys.* **8**, 470 (2020).
93. Gogioso, S. & Pinzani, N. The geometry of causality. Preprint at https://arxiv.org/abs/2303.09017 (2023).
94. Bong, K.-W. et al. A strong no-go theorem on the Wigner's friend paradox. *Nat. Phys.* **16**, 1199–1205 (2020).
95. Taddei, M. M., Nery, R. V. & Aolita, L. Quantum superpositions of causal orders as an operational resource. *Phys. Rev. Res.* **1**, 033174 (2019).
96. Chitambar, E. & Gour, G. Quantum resource theories. *Rev. Mod. Phys.* **91**, 025001 (2019).
97. Araújo, M., Guérin, P. A. & Baumeler, A. Quantum computation with indefinite causal structures. *Phys. Rev. A* **96**, 052315 (2017).
98. Chiribella, G. Perfect discrimination of no-signalling channels via quantum superposition of causal structures. *Phys. Rev. A* **86**, 040301 (2012).
99. Renner, M. J. & Brukner, Č. Computational advantage from a quantum superposition of qubit gate orders. *Phys. Rev. Lett.* **128**, 230503 (2022).
100. Bavaresco, J., Murao, M. & Quintino, M. T. Unitary channel discrimination beyond group structures: advantages of sequential and indefinite-causal-order strategies. *J. Math. Phys.* **63**, 042203 (2022).
101. Renner, M. J. & Brukner, Č. Reassessing the computational advantage of quantum-controlled ordering of gates. *Phys. Rev. Res.* **3**, 043012 (2021).
102. Buhrman, H., Cleve, R., Massar, S. & de Wolf, R. Nonlocality and communication complexity. *Rev. Mod. Phys.* **82**, 665–698 (2010).
103. Buhrman, H. R., Cleve, R. & Wigderson, A. Quantum vs. classical communication and computation. In *Proc. 30th Annual ACM Symposium on Theory of Computing* 63–68 (Association for Computing Machinery, 1999).
104. Raz, R. Exponential separation of quantum and classical communication complexity. In *Proc. Thirty-first Annual ACM Symposium on Theory of Computing* 358–367 (Association for Computing Machinery, 1999).
105. Baumeler, Ä. & Wolf, S. Perfect signaling among three parties violating predefined causal order. In *2014 IEEE International Symposium on Information Theory* 526–530 (IEEE, 2014).
106. Feix, A., Araújo, M. & Brukner, Č. Quantum superposition of the order of parties as a communication resource. *Phys. Rev. A* **92**, 052326 (2015).
107. Ebler, D., Salek, S. & Chiribella, G. Enhanced communication with the assistance of indefinite causal order. *Phys. Rev. Lett.* **120**, 120502 (2018).
108. Salek, S., Ebler, D. & Chiribella, G. Quantum communication in a superposition of causal orders. Preprint at https://arxiv.org/abs/1809.06655 (2018).
109. Wilde, M. M. *Quantum Information Theory* (Cambridge Univ. Press, 2013).
110. Chiribella, G. et al. Indefinite causal order enables perfect quantum communication with zero capacity channels. *N. J. Phys.* **23**, 033039 (2021).
111. Kristjánsson, H., Chiribella, G., Salek, S., Ebler, D. & Wilson, M. Resource theories of communication. *N. J. Phys.* **22**, 073014 (2020).
112. Chiribella, G. & Kristjánsson, H. Quantum Shannon theory with superpositions of trajectories. *Proc. R. Soc. Lond. A Math. Phys. Sci.* **475**, 20180903 (2019).
113. Procopio, L. M., Delgado, F., Enríquez, M., Belabas, N. & Levenson, J. A. Sending classical information via three noisy channels in superposition of causal orders. *Phys. Rev. A* **101**, 012346 (2020).
114. Procopio, L. M., Delgado, F., Enríquez, M., Belabas, N. & Levenson, J. A. Communication enhancement through quantum coherent control of *N* channels in an indefinite causal-order scenario. *Entropy* **21**, 1012 (2019).
115. Sazim, S., Sedlak, M., Singh, K. & Pati, A. K. Classical communication with indefinite causal order for *N* completely depolarizing channels. *Phys. Rev. A* **103**, 062610 (2021).
116. Caleffi, M. & Cacciapuoti, A. S. Quantum switch for the quantum internet: noiseless communications through noisy channels. *IEEE J. Sel. Areas Commun.* **38**, 575–588 (2020).
117. Abbott, A. A., Wechs, J., Horsman, D., Mhalla, M. & Branciard, C. Communication through coherent control of quantum channels. *Quantum* **4**, 333 (2020).
118. Guérin, P. A., Rubino, G. & Brukner, Č. Communication through quantum-controlled noise. *Phys. Rev. A* **99**, 062317 (2019).
119. Gisin, N., Linden, N., Massar, S. & Popescu, S. Error filtration and entanglement purification for quantum communication. *Phys. Rev. A* **72**, 012338 (2005).
120. Pang, A. O. et al. Experimental communication through superposition of quantum channels. *Quantum* **7**, 1125 (2023).
121. Lee, G., Hann, C. T., Puri, S., Girvin, S. M. & Jiang, L. Error suppression for arbitrary-size black box quantum operations. *Phys. Rev. Lett.* **131**, 190601 (2023).
122. Miguel-Ramiro, J. et al. Superposed quantum error mitigation. *Phys. Rev. Lett.* **131**, 230601 (2023).
123. Miguel-Ramiro, J. et al. Enhancing quantum computation via superposition of quantum gates. *Phys. Rev. A* **108**, 062604 (2023).
124. Spencer-Wood, H. Indefinite causal key distribution. Preprint at https://arxiv.org/abs/2303.03893 (2023).
125. Koudia, S., Cacciapuoti, A. S. & Caleffi, M. Deterministic generation of multipartite entanglement via causal activation in the quantum internet. *IEEE Access* **11**, 73863–73878 (2023).
126. Dey, I. & Marchetti, N. Entanglement distribution and quantum teleportation in higher dimension over the superposition of causal orders of quantum channels. Preprint at https://arxiv.org/abs/2303.10683 (2023).
127. Simonov, K., Caleffi, M., Illiano, J. & Cacciapuoti, A. S. Universal quantum computation via superposed orders of single-qubit gates. Preprint at https://arxiv.org/abs/2311.13654 (2023).
128. Zuo, Z., Hanks, M. & Kim, M. S. Coherent control of causal order of entanglement distillation. *Phys. Rev. A* **108**, 062601 (2023).
129. Chen, Y. & Hasegawa, Y. Indefinite causal order in quantum batteries. Preprint at https://arxiv.org/abs/2105.12466 (2021).
130. Guha, T., Alimuddin, M. & Parashar, P. Thermodynamic advancement in the causally inseparable occurrence of thermal maps. *Phys. Rev. A* **102**, 032215 (2020).
131. Guha, T., Roy, S., Simonov, K. & Zimborás, Z. Activation of thermal states by quantum SWITCH-driven thermalization and its limits. Preprint at https://arxiv.org/abs/2208.04034 (2022).
132. Simonov, K., Francica, G., Guarnieri, G. & Paternostro, M. Work extraction from coherently activated maps via quantum switch. *Phys. Rev. A* **105**, 032217 (2022).
133. Rubino, G., Manzano, G. & Brukner, Č. Quantum superposition of thermodynamic evolutions with opposing time's arrows. *Commun. Phys.* **4**, 251 (2021).
134. Rubino, G. et al. Inferring work by quantum superposing forward and time-reversal evolutions. *Phys. Rev. Res.* **4**, 013208 (2022).
135. Mancino, L., Sbroscia, M., Gianani, I., Roccia, E. & Barbieri, M. Quantum simulation of single-qubit thermometry using linear optics. *Phys. Rev. Lett.* **118**, 130502 (2017).
136. Mancino, L. et al. Geometrical bounds on irreversibility in open quantum systems. *Phys. Rev. Lett.* **121**, 160602 (2018).
137. Ball, P. A fridge without a cause. *Nat. Mater.* **21**, 1099–1099 (2022).
138. Capela, M., Verma, H., Costa, F. & Céleri, L. C. Reassessing thermodynamic advantage from indefinite causal order. *Phys. Rev. A* **107**, 062208 (2023).
139. Liu, X., Ebler, D. & Dahlsten, O. Thermodynamics of quantum switch information capacity activation. *Phys. Rev. Lett.* **129**, 230604 (2022).
140. Xi, C. et al. Experimental validation of enhanced information capacity by quantum switch in accordance with thermodynamic laws. Preprint at https://arxiv.org/abs/2406.01951 (2024).
141. Tang, H. et al. Demonstration of superior communication through thermodynamically free channels in an optical quantum switch. Preprint at https://arxiv.org/abs/2406.02236 (2024).
142. Frey, M. Indefinite causal order aids quantum depolarizing channel identification. *Quantum Inf. Process.* **18**, 96 (2019).
143. Ban, M. Quantum Fisher information of phase estimation in the presence of indefinite causal order. *Phys. Lett. A* **468**, 128749 (2023).
144. Chapeau-Blondeau, F. Noisy quantum metrology with the assistance of indefinite causal order. *Phys. Rev. A* **103**, 032615 (2021).
145. Kurdziałek, S., Górecki, W., Albarelli, F. & Demkowicz-Dobrzański, R. Using adaptiveness and causal superpositions against noise in quantum metrology. *Phys. Rev. Lett.* **131**, 090801 (2023).
146. Liu, Q., Hu, Z., Yuan, H. & Yang, Y. Optimal strategies of quantum metrology with a strict hierarchy. *Phys. Rev. Lett.* **130**, 070803 (2023).

147. Mothe, R., Branciard, C. & Abbott, A. A. Reassessing the advantage of indefinite causal orders for quantum metrology. *Phys. Rev. A* **109**, 062435 (2024).
148. Delgado, F. Parametric symmetries in architectures involving indefinite causal order and path superposition for quantum parameter estimation of Pauli channels. *Symmetry* **15**, 1097 (2023).
149. Zhao, X., Yang, Y. & Chiribella, G. Quantum metrology with indefinite causal order. *Phys. Rev. Lett.* **124**, 190503 (2020).
150. Giacomini, F., Castro-Ruiz, E. & Brukner, Č. Indefinite causal structures for continuous-variable systems. *N. J. Phys.* **18**, 113026 (2016).
151. Ban, M. Quantumness of qubit states interacting with two structured reservoirs in indefinite causal order. *Phys. Lett. A* **479**, 128927 (2023).
152. Gao, N. et al. Measuring incompatibility and clustering quantum observables with a quantum switch. *Phys. Rev. Lett.* **130**, 170201 (2023).
153. Pan, A. K. Leggett–Garg test of macrorealism using indefinite causal order of measurements. *Phys. Lett. A* **478**, 128898 (2023).
154. Krumm, M., Allard Guérin, P., Zauner, T. & Brukner, Č. Quantum teleportation of quantum causal structures. Preprint at https://arxiv.org/abs/2203.00433 (2022).
155. Quintino, M. T., Dong, Q., Shimbo, A., Soeda, A. & Murao, M. Reversing unknown quantum transformations: universal quantum circuit for inverting general unitary operations. *Phys. Rev. Lett.* **123**, 210502 (2019).
156. Quintino, M. T., Dong, Q., Shimbo, A., Soeda, A. & Murao, M. Probabilistic exact universal quantum circuits for transforming unitary operations. *Phys. Rev. A* **100**, 062339 (2019).
157. Quintino, M. T. & Ebler, D. Deterministic transformations between unitary operations: exponential advantage with adaptive quantum circuits and the power of indefinite causality. *Quantum* **6**, 679 (2022).
158. Yoshida, S., Soeda, A. & Murao, M. Reversing unknown qubit-unitary operation, deterministically and exactly. *Phys. Rev. Lett.* **131**, 120602 (2023).
159. Trillo, D., Dive, B. & Navascués, M. Universal quantum rewinding protocol with an arbitrarily high probability of success. *Phys. Rev. Lett.* **130**, 110201 (2023).
160. Oreshkov, O. Time-delocalized quantum subsystems and operations: on the existence of processes with indefinite causal structure in quantum mechanics. *Quantum* **3**, 206 (2019).
161. de la Hamette, A.-C., Kabel, V., Christodoulou, M. & Brukner, Č. Quantum diffeomorphisms cannot make indefinite causal order definite. Preprint at https://arxiv.org/abs/2211.15685 (2022).
162. Fellous-Asiani, M. et al. Comparing the quantum switch and its simulations with energetically constrained operations. *Phys. Rev. Res.* **5**, 023111 (2023).
163. Paunković, N. & Vojinović, M. Causal orders, quantum circuits and spacetime: distinguishing between definite and superposed causal orders. *Quantum* **4**, 275 (2020).
164. Ormrod, N., Vanrietvelde, A. & Barrett, J. Causal structure in the presence of sectorial constraints, with application to the quantum switch. *Quantum* **7**, 1028 (2023).
165. Vilasini, V. & Renner, R. Embedding cyclic causal structures in acyclic spacetimes: no-go results for process matrices. Preprint at https://arxiv.org/abs/2203.11245 (2022).
166. Saleh, B. E. A. & Teich, M. C. *Fundamentals of Photonics* 2nd edn (Wiley, 2007).
167. Felce, D., Vidal, N. T., Vedral, V. & Dias, E. O. Indefinite causal orders from superpositions in time. *Phys. Rev. A* **105**, 062216 (2022).
168. Cavalcanti, E. G., Chaves, R., Giacomini, F. & Liang, Y.-C. Fresh perspectives on the foundations of quantum physics. *Nat. Rev. Phys.* **5**, 1–3 (2023).
169. Hensen, B. et al. Loophole-free Bell inequality violation using electron spins separated by 1.3 kilometres. *Nature* **526**, 682–686 (2015).
170. Giustina, M. et al. Significant-loophole-free test of Bell's theorem with entangled photons. *Phys. Rev. Lett.* **115**, 250401 (2015).
171. Shalm, L. K. et al. Strong loophole-free test of local realism*. *Phys. Rev. Lett.* **115**, 250402 (2015).
172. Jamiołkowski, A. Linear transformations which preserve trace and positive semidefiniteness of operators. *Rep. Math. Phys.* **3**, 275–278 (1972).
173. Choi, M.-D. Completely positive linear maps on complex matrices. *Linear Algebra Appl.* **10**, 285–290 (1975).
174. Chiribella, G., D'Ariano, G. M. & Perinotti, P. Theoretical framework for quantum networks. *Phys. Rev. A* **80**, 022339 (2009).

Acknowledgements

This research was funded in whole, or in part, by the European Union (ERC, GRAVITES, no. 101071779) and its Horizon 2020 and Horizon Europe Research and Innovation Programme under grant agreement no. 899368 (EPIQUS) and no. 101135288 (EPIQUE) and the Marie Skłodowska-Curie grant agreement no. 956071 (AppQInfo). Views and opinions expressed are however those of the author(s) only and do not necessarily reflect those of the European Union or the European Research Council Executive Agency. Neither the European Union nor the granting authority can be held responsible for them. Further funding was received from the Austrian Science Fund (FWF) through 10.55776/COE1 (Quantum Science Austria), 10.55776/F71 (BeyondC) and 10.55776/FG5 (Research Group 5) and from the Air Force Office of Scientific Research under award number FA9550-21-1-0355 (QTRUST) and FA8655-23-1-7063 (TIQI); the financial support by the Austrian Federal Ministry of Labour and Economy, the National Foundation for Research, Technology and Development and the Christian Doppler Research Association is gratefully acknowledged. L.A.R. acknowledges support from the Erwin Schrödinger Center for Quantum Science and Technology (ESQ Discovery). B.-H.L. and Y.G. were supported by NSFC (no. 12374338 and no. 12204458) and China Postdoctoral Science Foundation (2021M700138 and BX2021289). This work benefitted from network activities through the INAQT network, supported by the Engineering and Physical Sciences Research Council (grant no. EP/W026910/1).

Author contributions

The authors contributed equally to all aspects of the article.

Competing interests

The authors declare no competing interests.

Additional information

Peer review information *Nature Reviews Physics* thanks Rafael Chaves and the other, anonymous, reviewer(s) for their contribution to the peer review of this work.